Heliyon 10 (2024) e33410

Contents lists available at ScienceDirect

Heliyon

journal homepage: www.cell.com/heliyon

Research article

Spatial analysis and mapping of intensity and types of agricultural salt-affected soils around Abaya and Chamo Lakes, South Ethiopia Rift Valley

Azmera Walche[a,b,*], Wassie Haile[b], Alemayehu Kiflu[b], Dereje Tsegaye[a]

[a] College of Agricultural Sciences, Arba Minch University, P.O. Box: 21, Arba Minch, Ethiopia
[b] College of Agriculture, Hawassa University, P.O. Box: 05, Hawassa, Ethiopia

A R T I C L E I N F O

Keywords:
Salt-affected soils
Intensity of salt problems
Types of salt
Geostatistical
Salinity and sodicity

A B S T R A C T

Purpose: Salt-affected soils have significant enough salt concentrations to impact other land and soil resource uses, plant health, soil characteristics, and water quality. Consequently, a study was carried out in the South Ethiopian Rift Valley area around the lakes of Abaya and Chamo to determine the intensity and the types of salt-affected soil and map their spatial distributions.
Methods: At 0–20 cm depths, a grid soil sampling scheme was employed to gather data from agricultural soils affected by salt. An adequately spaced grid cell of 200 m*200 m or seven transects, with seven samples collected every 200 m on each sampling site, was generated by the QGIS software's Fishnet tool, and an auger collected 226 soil samples from the proposed 245 soil sampling points. The analysis and interpretation of the data were done using both statistical and geostatistical methods. The un-sampled surface was predicted and mapped from laboratory point data using the standard Kriging algorithm in QGIS.
Results: According to the results, the soil in the study area was rated as strongly alkaline and moderately alkaline in the reaction. The coefficient of variation (CV) was the lowest for soil pH. Except for the Ganta Kanchama site, low CV (<10 %) confirmed the similarity of pH values throughout all research areas. The EC values depicted that the study area is slightly saline except for the Ganta Kanchame site, which rated moderately saline to strongly saline. The variability of soil EC rated moderate to strong variation for the studied area. The exchangeable sodium percentage (ESP) values distribution between the study sites demonstrates considerable variability and difference. The area is dominated by low to high-risk rate soil sodicity, as evidenced by the soil ESP CV of the studied area, which was >100 % and showed significant variability among the samples. Out of 2274.65ha of the studied area, the type of salt 62.28 %, 26.09 %, 10.99 %, and 0.63 % were categorized as non-saline non-sodic, saline-sodic, sodic, and saline, respectively. Following saline-sodic, sodic, and saline soils, respectively, non-saline and non-sodic soils comprise most of the investigated areas.
Conclusions: The result indicates almost all the salt-affected areas were situated in relatively lower slope areas exhibiting a flat to almost flat slope (0–2%). The study's findings are that the studied area needs specific soil management strategies to boost the salinity and sodicity problems around the study area and recommended reclamation techniques as the extent of the problems.

* Corresponding author.
E-mail address: azmera.walche@amu.edu.et (A. Walche).

https://doi.org/10.1016/j.heliyon.2024.e33410
Received 5 February 2024; Received in revised form 19 June 2024; Accepted 20 June 2024
Available online 22 June 2024
2405-8440/

1. Introduction

Different proportions of soils affected by salt can be found across all continents. Numerous attempts to quantify the global distribution of these soils may be found throughout the literature. Globally, salt-affected soils are a concern that lowers crop yields, soil sustainability, and cultivable land area [1–3]. Salt-affected soils are those with significant enough salt concentrations to have an impact on other land and soil resource uses, plant health, soil characteristics, and water quality [1]. According to some academics [4], it is also the term used to describe soils that have exchangeable sodium (sodicity), soluble salts, or both in proportions that can impede the growth and development of plants. In many nations, soil salinity and sodicity are the two main obstacles to agricultural production, which result in large losses in crop yield and land degradation [5,6]. The record of global extent of soil salinity is varied in literature [7]. For instance, according to Ref. [1], more than 120 nations worldwide have salt-affected soils, which vary in extent, nature and properties. Salinization currently poses a hazard to about 7 % of the world's land area [8]. According to Ref. [9], the problem of soil salinity is getting worse in North Africa, East Africa, the Middle East, East Asia, and South Asia, and it will get even worse in nations like America, China, Hungary, and Australia. According to a review of the global soil salinity by Ref. [4], 835 million hectares of land worldwide are affected by salt, with varying regional distributions.

It is commonly known that salt-affected soil occurs across Ethiopia. The areal extent of salt-affected soils encompass 11,033,000 ha of land in Ethiopia, most of which are located in the rift valley zone. Similar to this, the around Abaya and Chamo Lakes and Alage district's soil is impacted by salt in the rift valley zone of Ethiopia [10–13]. Soil salinization is a major environmental issue that can arise from both natural and human activity. High salt concentrations in parent materials or ground water result in primary salinization, a naturally occurring phenomenon that causes salts to build through natural processes [8,14,15]. According to Ref. [16], secondary salinization is a frequent result of excessive watering because of poor irrigation practices, poorly managed irrigation infrastructure, inadequate soil internal drainage, and improper irrigation water quality. Soil salinization is caused by soluble salts' upward movement and accumulation at or near the soil surface, which is facilitated by ground water [17]. Salts in the soil are transported with soil moisture by capillary action and become a cause of saline soil development when the water table is near the soil surface and the evaporation rate is high [18,19]. In agricultural soils, evapotranspiration causes salts to accumulate up in the root zone. This is because salts are left behind when water evaporates selectively through evapotranspiration [20]. Moreover, poor irrigation water quality, low soil permeability or a high water table can cause poor drainage [21], and topographic factors can cause an upslope recharge to cause a downslope outflow of salts, all of which can lead to an accumulation of soil salinity [22].

Based on research by Refs. [6,23], and others, soil salinity and sodicity development is generally a dynamic process with significant consequences for the soil, hydrological, agricultural, climatic, geochemical, social, and economic aspects. Soil salinity and sodicity are highly dynamic and varied spatially over time. A key management problem is the heterogeneity of the soil, which is primarily imposed by the mosaic distribution of salt and sodicity [24]. Different approaches to management and rehabilitation are predetermined by this variability. To enable site-specific management systems, spatial prediction, database setting up [25], and making digital maps of soil salinization and sodification patterns that can be used for action is very crucial [26]. Since the goal of developing and implementing successful soil reclamation programs is to prevent or reduce soil salinity and sodicity, data regarding the spatial extent, character, and distribution of soil salinity is becoming more and more crucial [27]. For agricultural management to be effective and to support site-specific management decisions, timely detection of soil salinity and sodicity as well as mapping of the spatial distribution and severity of salinity are crucial [28]. Prior to attempting any reclamation operations, mapping the types of salt-affected soils (saline, saline-sodic, and sodic) is the first step, as reclamation processes vary depending on the nature of the problem or its severity [29].

The two most popular GIS spatial interpolation techniques for forecasting and creating the spatial distribution map of soil properties like salinity are inverse distance weighting (IDW) and ordinary kriging [4]. Kriging is an accurate geostatistics technique that is commonly applied in various fields, including soil science [30,31]. Research by Ref. [13] found that the soil in the South Ethiopian Rift Valley surrounding Abaya and Chamo Lakes is prone to salinity and sodicity. Previous studies in this sector have been few and have primarily concentrated on taxonomic classification, soil characterization, and related topics due to the need for precise data regarding the extent and distribution of salt-affected soils in the region. It is essential to map the geographic distribution of salt-affected soil at each research site and determine its current condition. Agricultural productivity and environmental sustainability are seriously compromised by salt-affected soils, defined by high concentrations of soluble salts. Enabling informed decision-making and resource allocation for restoration and management options, mapping these soils offers an in-depth comprehension of their spatial distribution and extent. Therefore, identifying the various types of salt and the intensity of salt degradation is essential to managing and restoring soils damaged by salt. Decision-makers, researchers, and land managers can use this information to efficiently solve salt problems and advance environmentally friendly and sustainable farming practices. This would reduce further salinization and sodicity to sustain the agricultural lands through reclamation of the study area. Therefore, to support site-specific soil management tasks, strategies, and intervention, the study aimed to investigate the intensity and types of salt-affected soil and map their spatial distribution patterns around Abaya and Chamo Lakes in the South Ethiopia Rift Valley.

2. Materials and methods

2.1. Descriptions of the study area

The Abaya-Chamo sub-basin of the South Ethiopia Rift Valley that splits Ethiopia down the middle in a north-south direction. The basin comprises two lower-lying lakes, Abaya Lake and Chamo Lake [13,32]. The latitude of the study area falls between 5° 50′00″N and 6^0 10′ 0″N, and the Longitude of the study area falls between 37° 26′0″ E and 37° 40′0″ E. The altitude of the study area ranges from 1107 m around Chamo Lake to 1191 m at around Abaya Lake range. Besides this, the altitude of the Institutional University Cooperation (IUC) Project area ranges from 972 m around Abaya and Chamo lakes shores to 3464 m in the highland mountain range. The total area of the four watersheds is 807 km^2: Elgo (249 km^2), Sile (227 km^2), Baso (167 km^2), and Shafe (164 km^2). Elgo and Sile catchments drain Lake Chamo, whereas Baso and Shafe drain Lake Abaya. Of all Abaya-Chamo Lake watersheds, the area around two lower lying lakes, Abaya and Chamo Lakes, are selected for this specific study based on accessibility and the productive potential of the site for crop production and covered a 2019sq.km area (Fig. 1). Still, the specific sampling sites were selected based on the findings of the article of [13], which suggested detailed salinity and sodicity studies on the type, intensity, and distribution to specific sampling sites were recommended to apply the reclamation strategies in the study area. Accordingly, the Omo Lante, Lante, and Abulo sampling sites are located around Abaya Lake and Ganta Kanchama, and Zeyise Elgo sampling sites are located around Chamo Lakes South Ethiopia Rift Valley (Fig. 1) (appendix 1).

The climate around the Abaya and Chamo Lakes basin region is tropical, hot, and semi-arid [33]. The weather patterns in the Abaya-Chamo watersheds are, and it seems that the inter-tropical convergence zone (ITCZ) brings a humid breeze from the Indian Ocean that contributes to the bimodal rainfall system in the area. Altitude plays a role in the distribution of rainfall. The region experiences short rains in spring (belg) and long rains in summer (kremt), resulting in a bimodal rainfall distribution in most parts of the watershed [34]. In the study area, the rainfall peaks during April and May, with Chamo Lakes recording 152 mm and 133.5 mm, respectively, while around Abaya Lakes, the recorded rainfall is 146.5 mm and 118.5 mm. On the other hand, the lowest rainfall is recorded during January and February, with 9 mm and 20 mm for Chamo Lakes and 12.5 mm and 21.5 mm for around Abaya Lakes, respectively. The temperature is high for three months in the study area. For instance, around Chamo Lake, the temperature increases in February, March, and April, with 34.6°c, 35.1°c, and 33.9°c respectively. Around Abaya Lakes, the temperature is high during January, February, and March, with 31.4°c, 32.3°c, and 32.2°c, respectively. The mean annual rainfall in the area ranges from 500 to 1100 mm, and the average yearly air temperature is 17–39°c. According to the AMU-IUC Project 4 (Fig. 2), the mean soil temperature

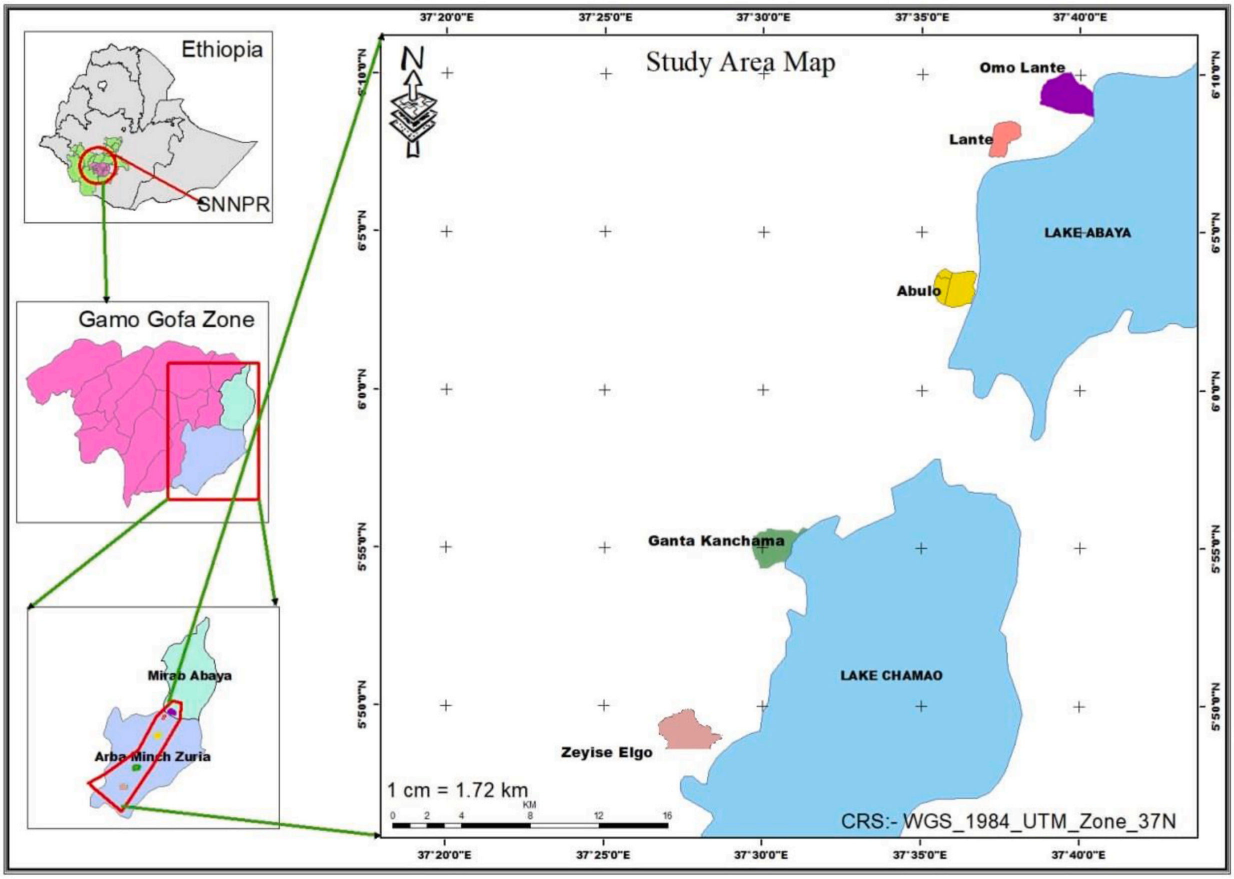

Fig. 1. Location map of the study sites. Where Omo Lante sampling site, which is the boundary between Omo Lante and Fura kebeles; Lante sampling sites, which represents Lante kebele; Abulo sampling sites, which are the boundaries between Shara kebele, Arba Minch University demonstration farm (AMU Demo Farm), and Abulo village; Ganta Kanchama sampling sites, which are the boundaries between Ganta Kanchama and Shele Mela kebeles; and Zeyise Elgo sampling site, which represents Zeyise Elgo kebele; SNNPR represents, South Nation Nationality People Region.

ranges from 22 to 35 °C depending on the depth (appendix 2). Agriculture seems to be dominant in the area, with crops such as banana, mango, papaya, maize, cotton, sweet potato, tomato, onion, and haricot beans being cultivated. However, it seems that soil salinity and sodicity are also present in the area. These phenomena are brought on by factors of nature such nearby or nearby water tables, weathering rocks and minerals, low rainfall and high evaporation rates. Unfortunately, these problems are made worse by human actions including inadequate irrigation, deforestation, and overgrazing of livestock [16].

2.2. Material used and soil sampling procedure

Measured field data (EC, ESP, and pH), soil, landform, and other maps, as well as additional data, were used together with the digital elevation model (DEM) at a resolution of 30 m. This investigation's Software tools include QGIS and Garmin GPS. The study area was demarcated from the Ethiopia Kebele administration boundary shape file and created a polygon layer for being studied. A grid sampling scheme was designed, and soil samples were collected from agricultural salt-affected soils around Abaya and Chamo Lakes South Ethiopia Rift Valley using an auger (appendix 3). It is one of the soil sampling strategies that deliver more information about the spatial distribution of salt-affected soil [19,35–37]. The QGIS software's Fishnet tool was utilized to create a grid of sampling points inside the polygon layer that were consistently spaced (appendix 4). A 200 m × 200 m grid cell was created, and nine (9) composite soil samples were taken from each grid node. Every composite soil sample was taken within a 15-m radius of the sampling point's center. An auger collected two hundred twenty-six (226) soil samples from 0 to 20 cm from the proposed 245 soil sampling points by 200 m × 200 m grid cell or seven transects, with seven samples collected every 200 m on each sampling site. We can estimate the total number of samples with the following formula: Total samples = Number of transects x Samples per transect. Total samples = seven (7) transects x 7 samples/transect, total samples = 49 samples for each sampling site, for five (5) sampling sites = 49*5 = 245. However, some sampling points fall on the mountains nearby, villages, and lakes around the sampling sites, then a total of 226 soil sampling points (Omo lante = 39, Lante = 44, Abulo = 48, Ganta Kanchama = 49, and Zeyize Elgo = 46) were used for this study (appendix 4). Before the field survey, the soil sampling point made by the Fishnet tool of the QGIS software was added to handheld GPS with coordinates for tracking the route and finding the sampling point. A global positioning system (GPS) was used to record the coordinates of each composite soil sampling point with an accuracy of ±3 m. Samples were taken accordingly, and their absolute locations were recorded. The collected samples were put in a clean plastic tray, crushed, mixed thoroughly, and transferred 1 kg composite soil sample to a plastic sampling bag.

2.3. Soil sample preparation and laboratory analyses

According to Ref. [38], field soil samples were dried by air at a suitable laboratory temperature of 24 °C in order to reduce soil mineralization. Soil samples were mechanically crushed with a mortar and pestle after drying, and then they passed through a 2-mm mesh sieve for laboratory analysis. Following a standard laboratory procedure, the collected soil samples have been determined for pH,

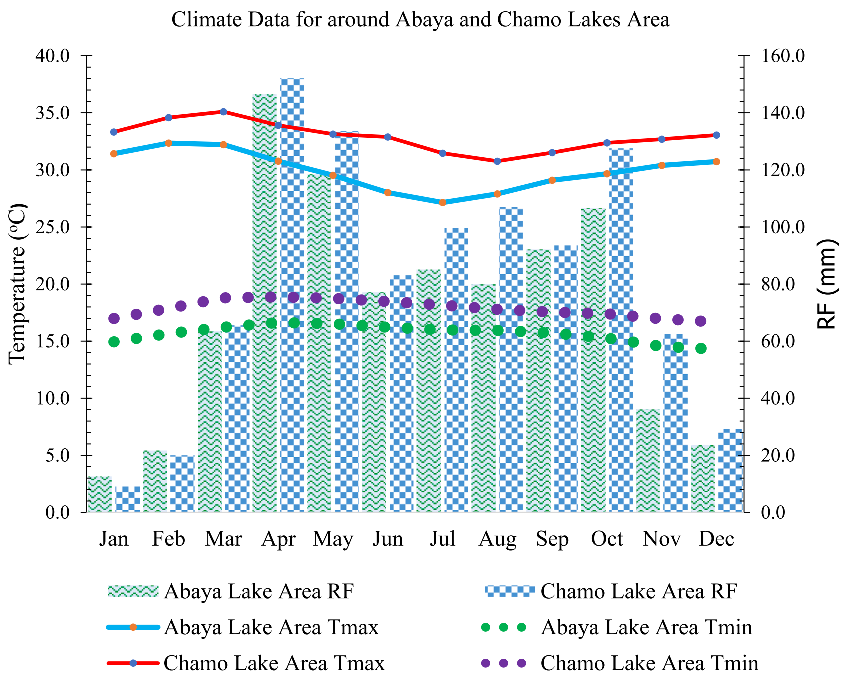

Fig. 2. Annual climate data around Abaya and Chamo lakes (1983–2020 average) where rain falls (RF) in millimetre (mm) and temperature (T) in degrees Celsius (^{0}C) (source: AMU-IUC project meteorology station).

exchangeable bases (Ca^{2+}, Mg^{2+}, K^+, and Na^+), and electrical conductivity (EC). A pH meter with a combined glass electrode in water (H_2O) was used to measure the pH of the soil at a ratio of 1:2.5 soil to water, in accordance with [39] recommendations. Saturated soil paste extracts were used to measure electrical conductivity using a conductivity meter, as described by Ref. [40]. The percolation tube method was followed by removing any excess ammonium ions from the soil solution by repeatedly washing it with 96 % ethanol after the exchangeable bases were determined using the 1M-ammonium acetate (pH 7) method [41]. The atomic absorption spectrophotometer was used to measure the exchangeable Ca^{2+} and Mg^{2+} from the extract and calculate the Ca and Mg saturation ratio. A flame photometer was used to determine the exchangeable K^+ and Na^+ from the same extracts, following [42] directions. The method described in Hand Book No. 60 was used to calculate the sodium adsorption ratio (SAR) and exchangeable sodium percentage (ESP) [43].

$$SAR = \frac{Na^+}{\left(\frac{Ca^{2+}+Mg^{2+}}{2}\right)^{\frac{1}{2}}} \tag{1}$$

$$\mathrm{ESP} = (100(-0.0126 + 0.01475(\mathrm{SAR})) / 1 + (-0.0126 + 0.01475(\mathrm{SAR}) \tag{2}$$

Finally, using [44] limit as a guide, the soil types affected by salt have been determined.

2.4. Land form

The Digital Elevation Model (DEM) of the study area was clipped from a 30 m resolution of Ethiopia in a GIS platform by masking QGIS software. The slope of the study area was generated from the Digital Elevation Model (DEM) of the study area in a GIS platform using surface analysis in QGIS software. The landform was used as one layer since landform features influence the process of salt accumulation on the soil surface due to its slope variability, which influences percolation and surface water flow [45]. Indirect features such as landscape may aid in identifying soil salinity and sodicity issues. The Combined action of topographic factors and climate has a significant influence on the spatial distribution of soil salinity, causing variations in soil salinity and sodicity distributions, particularly in arid areas [28,46,47].

Table 1
Descriptive statistics for selected soil properties around Abaya and Chamo Lakes.

Sampling site	Dis. Sta	Soil Parameters								
		pH	EC	Ex. Na	Ex. K	Ex. Ca	Ex. Mg	Ca: Mg	SAR	ESP
Omo Lante	N	39	39	39	39	39	39	39	39	39
	Min	7.30	0.38	0.40	0.08	17.43	5.73	0.37	0.07	0.30
	Max	8.57	6.13	78.45	11.46	51.72	47.69	7.33	13.75	19.21
	Mean	7.98	1.01	4.28	1.31	36.57	11.56	3.67	0.82	1.03
	Std. D	0.33	0.98	12.20	1.89	7.67	6.60	1.36	2.13	2.99
	CV%	4.14	96.62	285.11	144.85	20.98	57.11	37.07	258.80	289.47
Lante	N	44	44	44	44	44	44	44	44	44
	Min	8.04	0.34	0.07	0.08	11.23	4.44	0.68	0.02	0.73
	Max	9.64	4.68	75.72	16.78	47.37	40.94	4.63	17.84	25.31
	Mean	8.37	1.25	3.15	1.88	31.63	13.97	2.48	0.85	2.14
	Std. D	0.25	1.02	12.91	3.83	6.26	5.99	0.71	3.49	4.73
	CV%	2.94	81.81	409.26	203.73	19.78	42.89	28.65	411.34	220.58
Abulo	N	48	48	48	48	48	48	48	48	48
	Min	7.73	0.33	0.03	0.05	5.51	2.25	0.93	0.01	0.24
	Max	9.25	11.33	71.83	4.79	47.14	17.12	14.17	35.61	51.77
	Mean	8.33	1.69	5.26	0.85	29.25	9.46	4.33	1.88	2.88
	Std. D	0.26	2.22	13.01	0.92	10.70	4.84	3.52	5.82	8.31
	CV%	3.17	131.15	247.45	107.94	36.59	51.14	81.43	310.20	288.15
G/Kanchama	N	49	49	49	49	49	49	49	49	49
	Min	7.64	0.74	0.41	0.24	1.31	1.74	0.13	0.09	0.37
	Max	11.01	25.40	451.68	10.62	35.80	22.58	3.63	216.22	320.84
	Mean	8.82	4.22	158.96	2.78	19.92	12.13	1.67	51.24	75.63
	Std. D	0.92	4.93	144.99	2.28	9.16	4.19	0.71	54.97	81.37
	CV%	10.46	117.04	91.21	82.29	45.97	34.51	42.47	107.28	107.59
Zeyise Elgo	N	46	46	46	46	46	46	46	46	46
	Min	7.40	0.40	0.23	0.01	8.60	5.36	0.82	0.05	0.39
	Max	8.80	7.64	61.50	16.47	45.63	24.93	2.44	23.28	33.40
	Mean	8.16	1.43	6.18	1.23	28.44	16.27	1.80	1.63	2.60
	Std. D	0.28	1.44	11.93	2.39	6.41	4.60	0.33	3.88	5.28
	CV%	3.41	100.67	193.18	194.06	22.53	28.27	18.54	238.27	203.12

2.5. Cross-validation

The cross-validation was done to evaluate the accuracy of interpolation methods through mean error (ME), root mean square standardized error (RMSSE), and root means square error (RMSE). Closer values of the mean error (ME) to 0, and closer values of the root mean square standardized error (RMSSE) to 1, suggested that the prediction values were close to measured values, hence facilitating the selection of the best-fitted semivariogram model for an interpolation map, which could provide the most accurate predictions [48,49].

2.6. Data analysis

To analyze and interpret data, both statistical and geostatistical techniques were used. To analyze soil properties, descriptive statistics data were analyzed using SAS software, version 9.4 [50]. The coefficient of variation was used for the determination of soil properties variability. The variability is low when the CV is < 10 %, moderate between 10 and 100 %, and strong when > 100 % [51]. The rating and interpretation of determined values were based on a guide to standardized analytical methodologies for soil data. The spatial distribution of salt-affected soil in the study area was determined by importing the laboratory results into a GIS environment using their corresponding coordinates (latitude and longitude) in Microsoft Excel. Using interpolation techniques, the spatial prediction and mapping of the un-sampled surface from laboratory point values were carried out in a GIS environment. From laboratory point data, the un-sampled surface was predicted and mapped using the standard kriging algorithm in QGIS [52]. The map of the preliminary layers of the salt-affected soil indicator, including pH, EC, and ESP, and the predicted final salt-affected soil distribution map was generated.

3. Results and discussion

3.1. Descriptive statistics for salt-affected soil characteristics around Abaya and Chamo Lakes

Soil chemical properties are essential for developing different plants and crops [53]. Data presented in Table 1 shows the statistical summary of selected soil characteristics of agricultural salt-affected soils around Abaya and Chamo Lakes. This study evaluated the variables' dispersion using the coefficient of variation (CV) value. The CV in soil science can be categorized into three distinct categories. The variability is low when the CV is < 10 %, moderate between 10 and 100 %, and strong when > 100 % [51]. Among the soil properties analyzed, the coefficients of variation (CV) for Ex. Na^+, SAR, and ESP were the strong (Table 1). The coefficient of variation (CV) for soil pH was the lowest. Thus, low CV(<10 %) approved the similarity of pH values in all the study areas except the Ganta Kanchama site, which was categorized as moderate variability since the CV value is 10.46. As indicated in Table 1, the soil pH of the study area ranged from 7.30 to 8.57, 8.04 to 9.64, 7.73 to 9.25, 7.64 to 11.01, and 7.40 to 8.80, respectively, in the Omo Lante, Lante, Abulo, Ganta Kanchama, and Zeyise Elgo sites. According to US Salinity Laboratory Staff (1954) and [54] rating, the result depicted that the study area is characterized by non-alkaline to strongly alkaline to Omo Lante, Abulo, and Zeyise Elgo sites and moderately alkaline to strongly alkaline levels to Lante and Ganta Kanchama sites respectively.

The range values of EC varied from 0.38 to 6.13, 0.34 to 4.68, 0.33 to 11.33, 0.74 to 25.40, 0.40 to 7.64 dS m^{-1}, respectively, in the Omo Lante, Lante, Abulo, Ganta Kanchama, and Zeyise Elgo sites. According to soil quality standards given by Ref. [55], the result depicted that the study area is slightly saline except for the Ganta Kancheme site, which rated moderately saline to strongly saline. The CV of soil EC for the studied soils was between 10 % and 100 % for the Omo Lante and Lante sites and >100 % for the Abulo, Ganta Kanchama, and Zeyise Elgo sites. Based on [51] variability, the Omo Lante, and Lante were rated with moderate variation, and Abulo, Ganta Kanchama, and Zeise Elgo sites were rated with strong variation (Table 1). This variation of CV values for EC is supported by the findings of [30], who reported that low CV approved the similarity of soil properties, and high CV ratified the variations of soil properties.

The overall range values of ESP varied from 0.30 % to 19.21 % with a mean value of 1.03 %, 0.73–25.31 % with a mean of 2.14 %, 0.24 %–51.77 % with mean of 2.88 %, 0.37 %–320.84 % with mean value of 75.63 % and 0.39 %–33.40 % with mean of 2.6 %, in Omo Lante, Lante, Abulo, Ganta Kanchama and Zeyise Elgo sites (Table 1). The CV of soil ESP for the studied area was >100 %, indicating strong variability among the samples. However, the numerical CV (107.59) value of the Ganta Kanchama site revealed nearly moderate variability of ESP. This variation might be due to the difference in parent material, topographic position, drainage, groundwater table, temperature variation, soil texture variations, land use type, degree of removal of basic cations by crop harvest, and management types. This is supported by the finding of [56], who reported high water tables, insufficient soil permeability, inadequate drainage from irrigation systems, and topographic factors that cause an upslope recharge to cause a downslope salt outflow can all lead to an accumulation of soil salinity [57]. also found that land-use patterns, reclamation history, soil texture, and vegetation coverage were the most influential factors affecting spatial variation of soil salinity and sodicity.

The exchangeable Ca ranged from 17.43 to 51.72 cmol(+)/kg with a mean of 36.57 cmol(+)/kg, 11.23 to 47.37 with a mean value of 31.63 cmol(+)/kg, 5.51–47.14 cmol(+)/kg with a mean of 29.25 cmol(+)/kg, 1.31–35.8 cmol(+)/kg with a mean of 19.92 cmol (+)/kg, 8.6–45.63 cmol(+)/kg with a mean of 28.44 cmol(+)/kg in Omo Lante, Lante, Abulo, Ganta Kanchama, and Zeyise Elgo sites soils, respectively (Table 1). According to Ref. [55] rating, exchangeable Ca in the Omo Lante and Lante sites rated high to very high, and in Abulo and Zeise Elgo sites rated medium to very high, respectively, while in Ganta Kanchama Site rated very low to very high. The CV of soil exchangeable Ca for the studied soils was between 10 % and 100 % for the studied soils, which had moderate variability based on ratings of [51]. The exchangeable Mg ranged from 5.73 to 47.69 cmol(+)/kg with a mean of 11.56 cmol(+)/kg, 4.44 to 40.94

Table 2
Semivariogram models and model parameters for selected soil properties.

Soil Property			Fitted Model	Nugget (Co)	Partial Sill (C)	Sill	Range (m)	SPD	SPD Level	Estimated Error	
						(Co + C)		(Co/Co + C)*100		ME	RMSSE
Ex. Bases	pH		Sph	0.754	0.350	1.104	2875.2	68.297	Mo	−0.002	0.84
	EC		Exp	0.256	1.023	1.279	9101	20.016	St	0.098	0.551
		Ca^{2+}	Exp	0.198	0.855	1.053	15129	18.834	St	−0.035	0.96
		Mg^{2+}	Sph	0.748	1.130	1.878	1344	39.830	Mo	−0.001	1.157
		Na^{+}	Sph	0.425	0.516	0.941	3106	45.207	Mo	0.027	0.045
		K^{+}	Gau	0.230	0.990	1.220	7824	18.852	St	0.044	0.956
	SAR		Sph	0.369	0.553	0.922	3111	39.994	Mo	0.024	0.048
	ESP		Sph	0.388	0.441	0.829	4208	46.822	Mo	−0.169	1.181

Where: Mo = Moderate, St = Strong, Sph = Spherical, Gau = Gaussian, Exp = Exponential.

with a mean value of 13.97 cmol(+)/kg, 2.25–17.12 cmol(+)/kg with a mean of 9.46 cmol(+)/kg, 1.74–22.58 cmol(+)/kg with a mean of 12.13 cmol(+)/kg, 5.36–24.93 cmol(+)/kg with a mean of 16.27 cmol(+)/kg in Omo Lante, Lante, Abulo, Ganta Kanchama, and Zeyise Elgo sites soils, respectively (Table 1). According to Ref. [55] rating, exchangeable Ca in the Omo Lante, Lante, and Zyise Elgo sites rated high to very high, and in Abulo and Ganta Kanchama sites rated medium to very high, respectively. The CV of soil exchangeable Mg had moderate variability based on ratings of [51] since its range falls CV between 10 % and 100 % for the studied soils.

The Ca: Mg ratio is used to evaluate the potential impact of calcium on the uptake of Mg and P. As indicated in (Table 1) the soil Ca: Mg ratio of the study area varied from 0.37 to 7.33 ratio with a mean of 3.67 ratio, 0.68 to 4.63 with a mean value of 2.48 ratio, 0.93 to 14.17 ratio with a mean of 4.33 ratio, 0.13 to 3.65 ratio with a mean of 1.67 ratio, 0.82 to 2.44 ratio with a mean of 1.8 ratio in Omo Lante, Lante, Abulo, Ganta Kanchama, and Zeyise Elgo sites soils, respectively (Table 1). According to Ref. [55], when Ca: Mg ratios are less than 3:1, phosphorous (P) uptake may be inhibited, and it is suggested that the lowest acceptable limit with more subordinate Ca: Mg values, Ca availability slightly reduced [55]. Thus, the mean Ca: Mg ratio is less than 3:1 in the Lante, Abulo, Ganta Kanchama, and Zeyise Elgo sites where P uptake may be inhibited. In the Omo Lante site, the Ca: Mg ratio falls in the range of 3:1 to 4:1, which was the approximate optimum range for most crops, according to Ref. [55]. The CV of Ca: Mg was moderate variability in the study area.

The exchangeable Na ranged from 0.40 to 78.45 cmol(+)/kg with a mean of 4.28 cmol(+)/kg, 0.07 to 75.72 with a mean value of 3.15 cmol(+)/kg, 0.03–11.33 cmol(+)/kg with a mean of 5.26 cmol(+)/kg, 0.41–451 cmol(+)/kg with a mean of 158.96 cmol(+)/kg, 0.23–61.50 cmol(+)/kg with a mean of 6.18 cmol(+)/kg in Omo Lante, Lante, Abulo, Ganta Kanchama, and Zeyise Elgo sites soils, respectively (Table 1). According to Ref. [54] rating, exchangeable Na in the Omo Lante and Ganta Kanchama sites rated medium to very high, and in the Lante and Abulo sites rated very low to very high, respectively, while the Zeyise Elgo Site rated low to very high. The CV of soil exchangeable Na for the studied soils had strong variability except for the Ganta Kanchama site, which had moderate variability based on the ratings of [51].

3.2. Geostatistical analysis and mapping of selected soil properties

The spatial attribute is defined by the nugget/sill ratio or spatial dependence (SPD) Co/(Co + C). When the value of Co/(Co + C) is less than 0.25, the variable is said to have a strong spatial dependency; when it is between 0.25 and 0.75, it is considered to have a moderate geographic dependence; and when it exceeds 0.75, it is considered to have a weak spatial dependence [48,49,58,59]. Table 2 shows the semivariogram obtained from the geostatistical study, illustrating the various geographical distribution models and levels of

Table 3
The areal extent of the different classes of selected soil chemical properties with respect to sampling sites.

Soil properties	Rating	Status	Soil sampling sites									
			Omo Lante		Lante		Abulo		Ganta Kanchama		Zeyise Elgo	
			Area (ha)	Area (%)	Area (ha)	Area (%)	Area (ha)	Area (%)	Area (ha)	Area (%)	Area (ha)	Area (%)
EC	<4	Non-Saline	558.01	99.71	250.49	99.36	420	96.11	263.46	42.35	422.01	98.83
	4–8	Slightly-Saline	1.64	0.29	0.6	0.24	16	3.66	339.82	54.62	5	1.17
	8–15	Moderately Saline	–	–	–	–	1	0.23	16.07	2.58	–	–
	>15	Strongly Saline	–	–	–	–	–	–	2.78	0.45	–	–
ESP	<5	Low	553.86	98.97	232.94	92.77	419.36	95.96	4.59	0.74	420	98.36
	5–15	Medium	5.18	0.93	14.15	5.63	10.81	2.47	15.54	2.5	5.01	1.17
	>15	High	0.62	0.11	4	1.59	6.7	1.53	601.98	96.76	2	0.47
pH	7.5–8.5	Moderately alkaline	558.6	99.81	232.8	92.71	109.25	25.00	246.89	39.69	427	100
	>8.5	Strongly alkaline	1.5	0.19	18.29	7.29	327.75	75.00	375.23	60.32	0.1	0.02
Ex_Na	<0.10	Very Low	–	–	0.47	0.19	4.43	1.01	–	–	–	–
	0.1–0.3	Low	–	–	28.38	11.3	27.99	6.41	–	–	–	–
	0.3–0.7	Medium	0.03	0.01	146.38	58.3	18.98	4.34		–	0.3	0.07
	0.7–2.0	High	6.1	1.09	12.91	5.14	181.11	41.44	0.13	0.02	0.7	0.16
	>2.0	Very High	553.56	98.9	62.94	25.07	204.37	46.77	621.99	99.99	426	99.76
Ex_Ca	2–5	Low	–	–	–	–	–	–	1.32	0.21	–	–
	5–10	Medium	–	–	–	–	3.18	0.73	10.34	1.66	–	–
	10–20	High	0.33	0.06	1.57	0.63	23.19	5.31	177.58	28.55	0.01	0.02
	>20	Very High	559.32	99.94	249.52	99.37	410.51	93.94	432.77	69.58	426.57	99.99
Ex_K	<0.2	Very Low	0.38	0.07	1.01	0.4	7.72	1.77	–	–	0.5	0.12
	0.2–0.5	Low	9.86	1.76	57.47	22.89	101.1	23.14	0.32	0.05	0.5	0.12
	0.5–1.5	Optimum	504.06	90.05	185.41	73.85	301.08	68.9	38.24	6.15	152	35.6
	1.5–2.3	High	30.16	5.39	7.17	2.86	26.92	6.16	153.9	24.74	230	53.86
	>2.3	Very High	15.3	2.73	–	–	–	–	429.7	69.07	44	10.3
Ex_Mg	1.51–3.3	Medium	–	–	–	–	40.31	9.22	0.7	0.11	–	–
	3.31–8.3	High	15.69	2.8	1.08	0.43	92.23	21.1	11.68	1.88	0.07	0.02
	>8.31	Very High	543.96	97.2	250.02	99.58	304.3	69.63	609.73	98.01	426.53	99.98

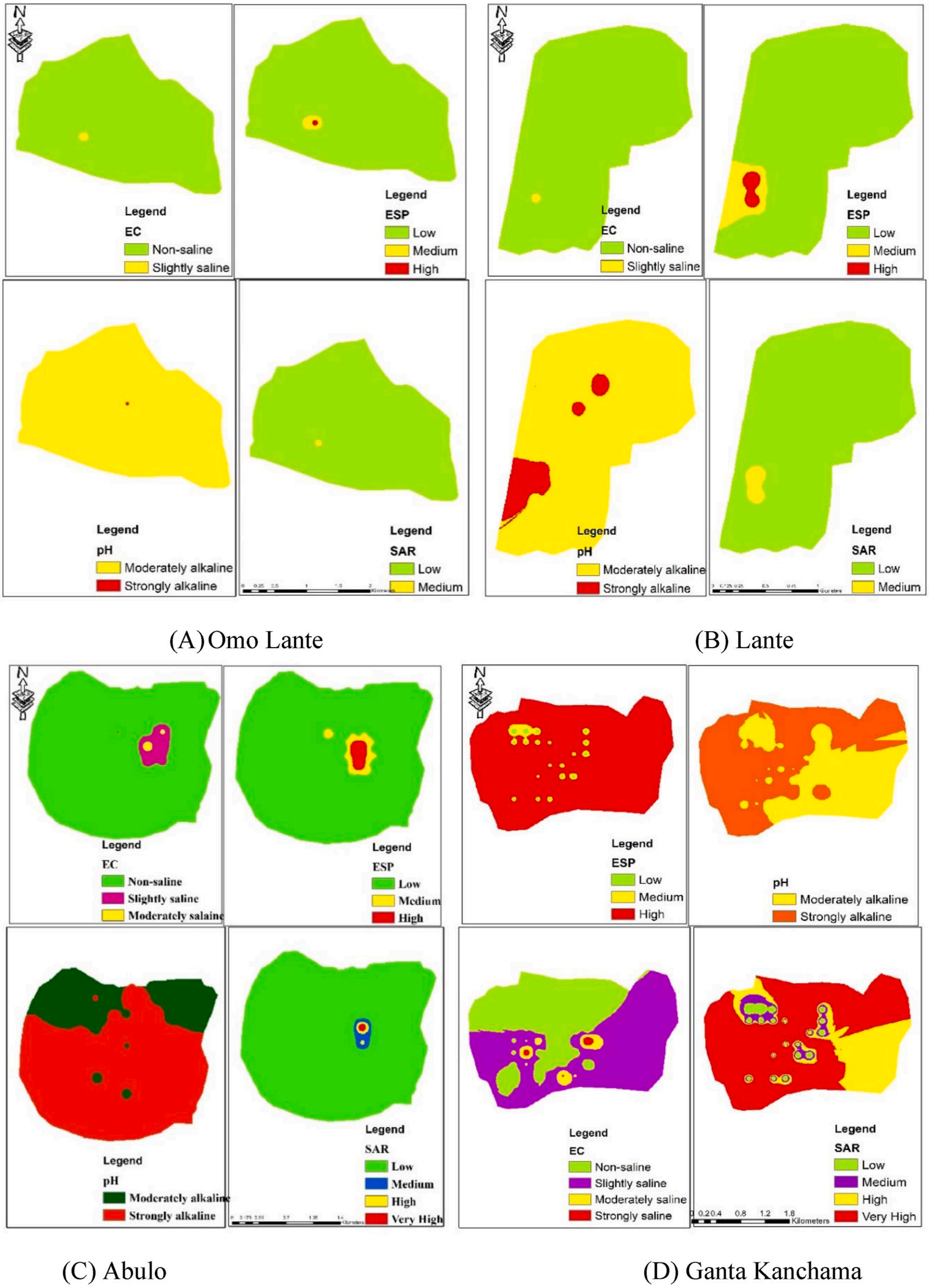

Fig. 3. This figure shows the spatial distribution map of the study area's pH, EC, ESP, SAR, and Exchangeable bases. Where (A) Omo Lante, Which is represented by the Omo Lante sampling site, shows the intensity and spatial distribution map of EC, pH, ESP, and SAR. (B) Lante: It represents the Lante sampling site and shows the intensity and spatial distribution map of EC, pH, ESP, and SAR. (C) Abulo: The Abulo sampling site shows the

intensity and spatial distribution map of EC, pH, ESP, and SAR. (D) Ganta Kanchama: The Ganta Kanchama sampling site shows the intensity and spatial distribution map of EC, pH, ESP, and SAR. (E) Zeyise Elgo: This is represented by the Zeyise Elgo sampling site and shows the intensity and spatial distribution map of EC, pH, ESP, and SAR. (F) Omo Lante: Which is represented by the Omo Lante sampling site, shows the intensity and spatial distribution map of Exchangeable bases (Na, K, Ca, and Mg).

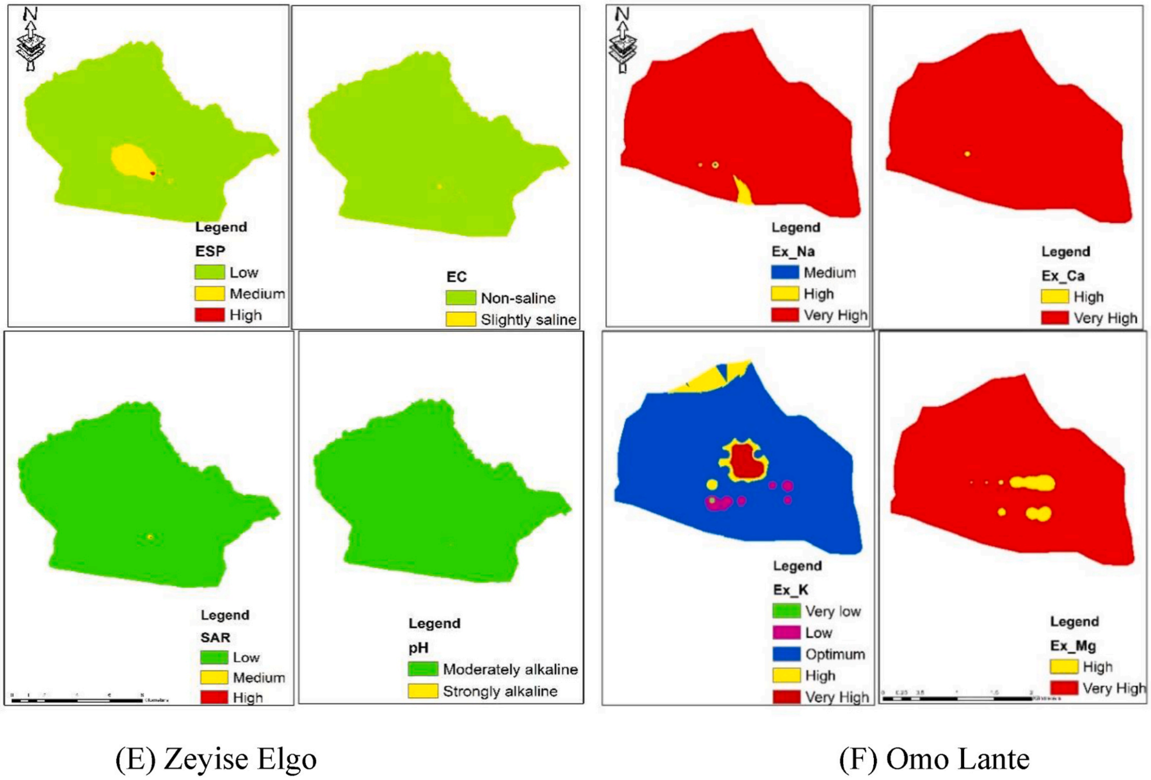

Fig. 3. (*continued*).

spatial dependency associated with the soil parameters. Semivariance revealed variations in the spatial dependence of soil parameters (Table 2). The nugget-to-sill ratio [Co/(Co + C)] of [pH, Mg, Na, SAR, and ESP] ranged from 0.25 to 0.75, as shown in Table 2, suggesting a moderate spatial dependence.

This implies that the properties were controlled by both intrinsic and extrinsic factors. It could be the continuous use of salt-affected irrigation water on the field, cultivation practices including plowing, fertilization, and other soil management practices [58,60–62]. This is in agreement with the findings of [63] who reported that moderate spatial dependence is due to both intrinsic and extrinsic factors. According to Ref. [49], the nugget/sill ratio (C0/C0 + C) < 25 % reflected a strong spatial dependence of [EC, Ca, and K]. The results of the distribution were explained by the model which shows to be affected by natural factors which are mostly geological in nature. This could be mainly due to the inherent/intrinsic sources of variability (e.g., natural variations in soils, such as soil texture, parent materials, and topography) [64]. The majority of the researchers also stated that random extrinsic factors like soil management techniques like fertilization and plowing are related to weak spatial dependency, while strong spatial dependency is related to structural intrinsic factors like parent material, mineralogy, texture, climate, and topography. Conversely, a considerable degree of spatial dependence is probably influenced by both extrinsic and intrinsic variables [65–67]. For soil EC, the nugget effect was typically higher (Table 2). This indicated that differences in soil qualities existed at short distances. The spatial variability at smaller distances than the lowest separation between measurements is associated with the nugget effect [64,68].

The results indicated that the mean errors (ME) were near zero and the root mean square standardized error (RMSSE) was close to 1 for all studied soil parameters (Table 2). The result is similar to the finding of [66] who reported closer values of the mean error (ME) to 0, and closer values of the root mean square standardized error (RMSSE) to 1, suggesting that the prediction values were close to measured values, hence providing the most accurate predictions.

A wider range value means that different values of the soil property over longer distances have an impact on the observed values of this property [64,69]. As indicated in Table 2, the spatial range values for all studied soil properties varied from 1344 m to 15,129 m, which is greater than the average sampling distance (200 m), implying that the sampling interval in this study was sufficient to capture the spatial variability in studied soil properties. Thus, results indicate the sampling strategy was adequate. Similarly [70], reported that if the range value is greater than the actual sampling distance, the sampling strategy is adequate to capture the spatial variability of studied soil properties.

3.3. Spatial distribution map of selected soil chemical properties

3.3.1. Mapping the spatial distribution of soil pH

The area calculated from the interpolated map of salt-affected soil parameters created from measured point data is presented in Table 3, and its spatial distribution is shown in Fig. 3. According to the US Salinity Laboratory Staff [43] rating, the interpolation result depicted that the study area is moderately alkaline to strongly alkaline (Table 3). The area calculated from the predicted map shows that 558.6ha (99.8 %), 232.8ha (92.71 %), 327.75ha (75 %), 375.25ha (60 %), and 427ha (100 %), respectively, for Omo Lante, Lante, Abulo, Ganta Kanchama, and Zeyise Elgo sampling sites. The studied area had pH values greater than 8.5 for Omo Lante, Abulo, and Ganta Kanchama and between 7.5 and 8.5 for Lante and Zeyise Elgo (Table 3 and Fig. 3). It was rated as strongly alkaline and moderately alkaline in the reaction, respectively, according to the US Salinity Laboratory Staff [71] rating, indicating that a significant portion of the studied area requires alkalinity management practices. The studied area has a pH value greater than 7.5 (Table 3 and Fig. 3). This showed that alkaline soils dominate the study area. In the case of the Abaya and Chamo Lakes region, the low rainfall and high evaporation rates are likely the primary factors contributing to the increased alkalinity of the soils. The area is in a semi-arid climate, with an average annual rainfall of less than 600 mm. However, the evaporation rate is very high due to the hot and dry environment [13,72] This leads to the accumulation of salts in the soil, which can make it alkaline. The strongly alkaline soils may be attributed to low leaching of bases, especially in clay soils [55,73]. The application of poor-quality water would increase pH. This might be due to the continuous irrigation practices with salt-affected irrigation water and shallow ground water table that happened in the [13,19]. This result is supported by the findings of [74–76] that alkalinity in arid and semi-arid areas is caused by irrigation water. The reason for this is that irrigation water can gradually introduce more salts into the soil by evaporating water and concentrating the dissolved salts in the soil solution [77,78]. In addition to this, additional factors may contribute to the alkalinity of the study soils since it is in the Rift Valley, a region of volcanic activity, and the volcanic ash that has fallen over the area is often alkaline. Some fertilizers, such as lime and urea, can make the soil more alkaline, and some minerals, such as sodium bicarbonate and sodium carbonate, release alkaline ions when they dissolve in water [79–81]. The high alkalinity of the soils around Abaya and Chamo Lakes can negatively impact agriculture. Alkaline soils can reduce crop yields, make it difficult for plants to absorb nutrients, and increase disease risk [82, 83].

3.3.2. Mapping the spatial distribution of soil electrical conductivity (EC)

Fig. 1 shows the soil EC map generated by interpolating the point data result. There was substantial variation in soil electrical conductivity (EC) in various parts of the research area, as indicated by the area computed based on the projected map. About 558.01 ha (99.71 %), 250.49 ha (99.36 %), 420 ha (96.11 %), and 422.01 ha (98.93) of the studied soils had EC values less than 4 dS/m (Table 3), respectively, for Omo Lante, Lante, Abulo, and Zeyise Elgo. These soils were generally categorized as free of excess salt, having no adverse effect on the growth and productivity of most crops according to the soil quality standards established by Refs. [54,55]. Table 3 shows that EC values for 339.82ha (54.60 %) and 428.36 ha (57.38 %) were between 4 and 8 dS/m. These values could be rated slightly saline soil class throughout the studied area (Fig. 3). One of the leading causes of soil salinization and sodicity in the area is the irrigation of agricultural land with subsurface and river water for more than 15 years. Salts may be brought to the soil's surface by irrigation water over time, where they can accumulate and harm crops. This is especially true in dry and semi-arid areas with little precipitation and considerable evaporation [84,85]. It is encouraging that most of the studied agriculturally salt-affected soil area is non-saline and non-sodic. It implies that there is still time to take action to prevent further damage and that the problem still needs to be severe [86,87]. According to the soil EC maps, it is incredibly reassuring to see that non-saline and slightly saline soils are mainly concentrated throughout the entire study area [88,89]. It indicates that successful crop cultivation is still possible in various locations. The following recommendations can be used to reduce soil salinization and sodicity in agricultural areas: Grow salt-tolerant crops, drain the soil frequently to eliminate accumulated salts, and use irrigation water wisely and effectively [90]. Incorporate organic matter into the soil to enhance water retention and drainage, and use gypsum to improve soil structure [91].

3.3.3. Mapping the spatial distribution of soil ESP

The distribution pattern of ESP values is shown in Fig. 3. The distribution of ESP values shows a substantial difference in the study area. The spatial interpolation result (Fig. 3) indicated a considerable variation in soil ESP across different parts of the study area. The spatial interpolation result (Fig. 3) suggested that the area is dominated by soil sodicity of low to high risk rated according to Ref. [55]. In terms of risks, 553.86ha (98.97 %), 232.94ha (92.77 %), 419.36ha (95.96 %), and 420ha (98.36 %) of the studied area for Omo Lante, Lante, Abulo and Zeise Elgo sampling sites is classified under low (ESP <5 %) risks of sodicity, respectively (Table 3 and Fig. 3). Under the low-risk level of ESP (<5 %), those sampling sites could be medium to high soil exchangeable calcium amounts. A high sodicity problem area with ESP (>15 %) was observed in the Ganta Kanchama sampling site of the study area (Table 3 and Fig. 3). The highest ESP (>15 %) values were concentrated in the Ganta Kanchama sampling site of the studied area due to the higher exchangeable sodium found in the soil of these sampling sites (Fig. 3). These may result from the relatively high clay content of soils in this study area site. The higher ESP results in this area are most likely due to the relatively high clay content of the soils in the Ganta Kanchama sampling site [13]. Because clay particles have a large surface area, there are more sites for sodium ions to bind to them. Furthermore, in sodic soils, certain clay minerals, including smectite, are especially prone to dispersion [92,93]. Smaller clay particles that are released into the soil have the potential to clog soil pores. This decreased water and air uptake may impede plant growth into the soil [89]. Additionally, plants may find getting nutrients from sodic soils challenging due to their high sodium level [94]. It is very encouraging that the study area is dominated by low to high-risk soil sodicity. This means that the area is generally suitable for crop production [30,95]. However, there is a need to manage and follow up on the status of the soil properties to ensure that the area

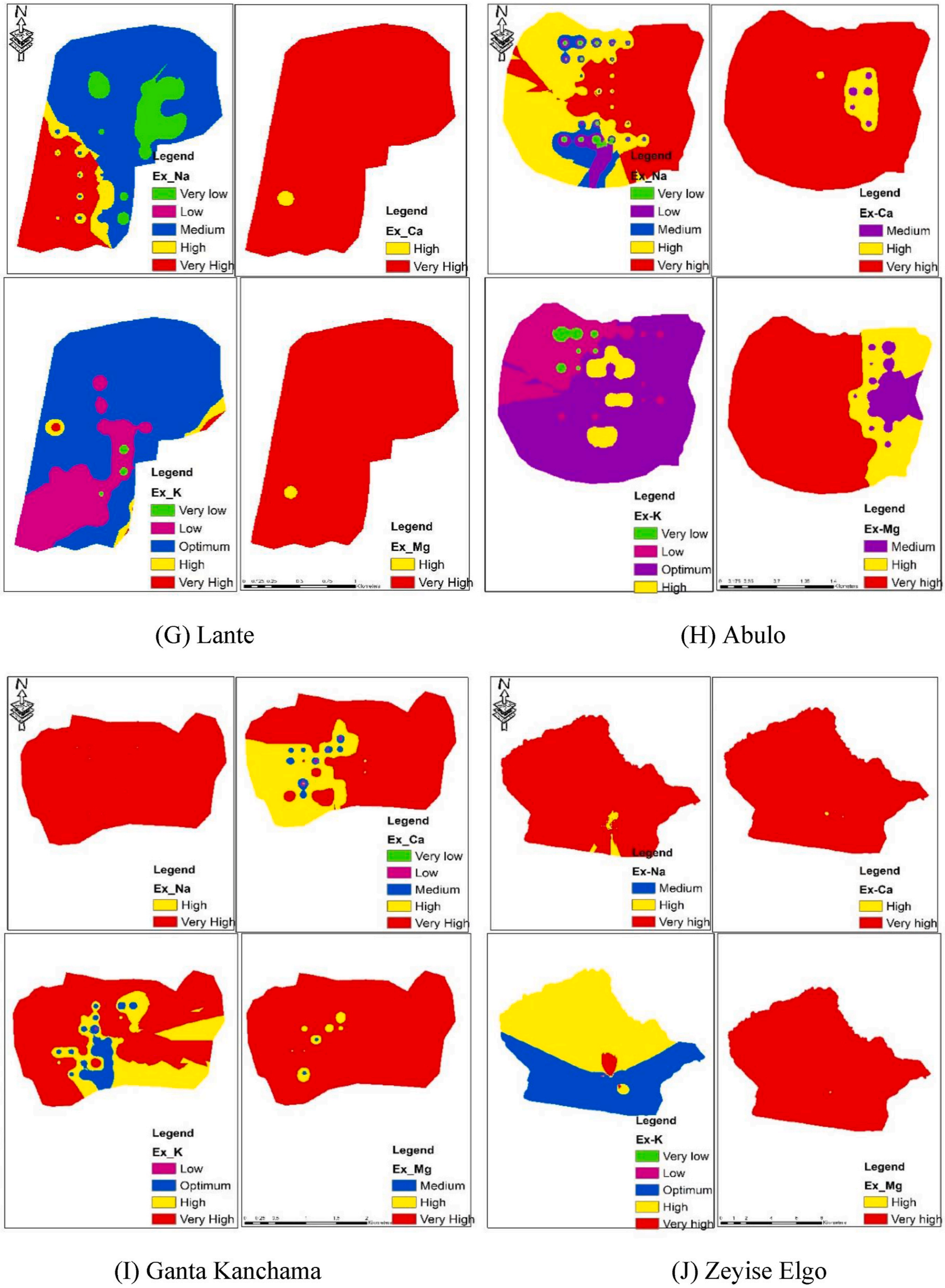

Fig. 4. This figure shows the study area's intensity and spatial distribution map of exchangeable bases (Na, K, Ca, and Mg). Where (G) Lante, (H) Abulo, (I) Ganta Kanchama, and (J) Zeyise Elgo sampling sites, respectively, in the study area.

remains favorable for crop growth. Here are some specific things that can be done to manage and follow up on the status of soil properties in the study area: monitor soil sodicity levels, maintain soil organic matter levels, use irrigation water that is low in sodium, and manage irrigation practices carefully. It is also important to select crops that are tolerant of soil sodicity [47,96–98].

3.3.4. Mapping the spaial distribution of exchangeable sodium

Fig. 4 depicts the distribution pattern of exchangeable sodium values. There is a noticeable variation in the exchangeable sodium value distribution within the research area. There was an important variation in soil exchageable sodium in different areas of the research region, according to the spatial interpolation result (Fig. 4). As per [55], the spatial interpolation result (Fig. 4) revealed that exchangeable sodium with a high rate dominates the area. The Omo Lante(Fig. 3), Abulo, Ganta Kanchama, and Zeise Elgo sampling sites have very high exchangeable sodium amounts in terms of area, with classifications of 553.56ha (98.9 %), 204.37ha (46.77 %), 621.99ha (99.99 %), and 426ha (99.76 %); the exchangeable sodium amount of the Lante sampling site, on the other hand, was rated as medium by Refs. [54,55] (Table 3 and Fig. 4). It is evident that the research area's soil exchangeable sodium varies significantly, with much of it having very high levels of exchangeable sodium. This is probably caused by a number of factors, such as land use, soil type, and climate [99,100]. There are several detrimental effects that high exchangeable sodium levels may have on soil health and plant growth. Waterlogging and root rot can result from exchangeable sodium's potential to decrease soil permeability and aeration [101,102]. Additionally, it may make nutrient loss and soil erosion more likely. To make sure that the management strategies work, it's critical to periodically monitor the soil's Na level [103–105].

3.3.5. Mapping the spaial distribution of exchangeable calcium

There was a slight variation in soil exchangeable calcium in different areas of the research region, according to the spatial interpolation result (Fig. 3). The results of the investigation show that, overall, the soil exchangeable calcium in the study area is very high. The Ganta Kancham sampling site, on the other hand, was rated by Ref. [55] to range between low and very high. According to Refs. [54,55], the Omo Lante (Fig. 3), Lante, Abulo, Ganta Kanchama, and Zeise Elgo sampling sites have very high exchangeable calcium amounts in terms of area, about 559.32ha (99.9 %), 249.52ha (99.37 %), 410.51ha (93.94 %), 432.77ha (69.58 %), and 426.5 (99.99 %) respectively(Table 3 and Fig. 4). The findings suggest that the Ganta Kancham sampling site should be amended with calcium-rich amendment materials, like gypsum and organic materials, to increase the availability of calcium, since according to Refs. [106,107], calcium is an essential nutrient for plant growth and development. However, the findings also note that the exchangeable calcium amount is generally sufficient for crop production if the exchangeable sodium is managed regularly. Exchangeable sodium is a harmful ion that can displace calcium from the soil exchange complex, making it unavailable to plants [108–110]. Therefore, it is essential to monitor the soil's exchangeable sodium levels and apply appropriate management practices to reduce sodium levels, such as leaching and gypsum. This will help ensure the soil has sufficient calcium for crop production [111–113].

3.3.6. Mapping the spaial distribution of exchangeable magnesium

There was a variation in soil exchageable magnesium in different areas of the research region, according to the spatial interpolation result (Fig. 4). The findings of the study indicates that the soil exchangeable magnesium in the study area is generally very high, with the exception of the Abulo sampling site which was rated medium to very high according to the rating of [55]. The Omo Lante (Fig. 3), Lante, Abulo, Ganta Kanchama, and Zeise Elgo sampling sites have very high exchangeable calcium amounts in terms of area, with classifications of 543.96ha (97.2 %), 250.02ha(99.58 %), 304.3ha(69.63 %), 609.73ha (98.01 %), and 426.53 (99.98 % respectively according to Refs. [54,55] (Table 3 and Fig. 4). The research region exhibits high levels of soil exchangeable magnesium, with all sites except Abulo sampling site rated as medium to very high. These factors, including divalent cations like magnesium and calcium, are essential for plant growth [114,115]. This allows them to bind to negatively charged clay particles in the soil [116,117]. The combination of high soil pH, limited rainfall, and parent material rich in calcium is probably what causes the raised calcium levels [118]. The similar trends in distributions, interpolations, and ratings of these nutrients suggest that similar factors control these nutrients, aiding farmers and land managers in better soil fertility and crop production [119,120].

3.3.7. Mapping the spaial distribution of exchangeable potasium

Fig. 4 shows the soil exchangeable potassium map generated by interpolating the point data result. Variation in soil exchangeable potassium in various parts of the research area, as indicated by the area computed based on the projected map. Generally, the study area's exchangeable potassium values were rated in the range of optimum to very high. About 504.06 ha (90.05 %), 185.41 ha (73.85 %), 301.08 ha (68.9 %), and 429.7ha (69.07) of the studied soils were rated optimum exchangeable potassium (0.5–1.5 cmol(+)/kg) amount and very high (>2.3 cmol(+)/kg) for Omo Lante (Fig. 3), Lante, Abulo, and Ganta Kanchama sites respectively, while for Zeyise Elgo site 230 ha (53.86 %) area had exchangeable potassium values between 1.5 and 2.3 cmol(+)/kg, was rated high according to Refs. [54,55] (Table 3 and Fig. 4). The parent material that the soils in the study area formed is probably what causes the raised potassium levels there. The Rift Valley is a volcanically active location, and the fallen volcanic ash contains a lot of potassium. Moreover, the Rift Valley's typically alkaline soils help to better retain potassium [10,121]. Potassium is required for photosynthesis, disease resistance, and fruit production. Among the crops that respond well to potassium are sweet potatoes, potatoes, and bananas [122,123]. The overall results of the study indicate that the high potassium levels in the soils of the Abaya and Chamo Lakes in the South Ethiopian Rift Valley seem to make them generally suitable for crop growth [13,82]. It is important to keep in mind that a number of variables, such as soil pH, organic matter content, and nutrient availability, influence crop growth. Farmers in the research area should test their soil to apply fertilizers based on the precise nutritional requirements of their crops [124,125].

3.4. Mapping the spatial distribution of salt-affected areas

The distribution of salt-affected soil in the studied area showed spatially heterogeneous patterns throughout the studied area. The classified salt-affected soils by Ref. [44] revealed that the studied area is classified as neutral (non-saline non-sodic), saline, saline-sodic, and sodic. Results showed that 558.01ha (99.71 %), 419.4ha (96 %), and 420ha (98.36 %) of Omo Lante site, Abulo, Zeyise Elgo site soil of the study area were found to be non-saline non-sodic. While 228.71ha (99.98 %) and 352.69ha (56.65 %) of the Lante site and Ganta Kanchama studied areas were found to be saline-sodic soils, respectively. The Ganta Kanchama site of 249.51ha (40.1 %) was sodic soil (Table 4 and Fig. 5). From all sampling sites, the Ganta Kanchama site was found to be affected severely, recording 602.96ha (97.54 %) (Table 4 and Fig. 5). The Ganta Kancham site had heavy clay soil texture, high temperature and shallow ground water table which can facilitate the soil salinity and sodicity formation in the study area [13]. Similarly, shallow groundwater depth has a higher influence on soil salinity rise and a higher depth of groundwater level has a lower influence on soil salinization. A shallow ground water table leads to high capillary movement of water and increases the risk of salinization [19,126]. Due to capillary action, the salts in the soil are carried by soil moisture and contribute to the production of salty and sodic soil when the water table is near the soil's surface and the rate of evaporation is high [127,128]. The result indicates that the type of salt 1416.76ha (62.28 %), 593.57ha (26.09 %), 250.15ha (10.99 %), and 14.16ha (0.63) were categorized according to Ref. [44] to non-saline non-sodic, saline-sodic, sodic and saline respectively. Thus, non-saline, non-sodic soils take the most significant part of the total 2274.64 ha studied area (Table 4 and Fig. 5).

3.5. Salt-affected soil type and distribution with respect to land form

As indicated in Fig. 5 sodic and saline soils area laid on a relatively flat area in <0–5% in deep red and light red, respectively. Saline soils also found in the slope range 1–2% and slope range 0.5–1% in orange and deep yellow color respectively as show in Fig. 5. Most non-saline non-sodic soils was found the slope <2 % as showed in the figure with different colors. The result indicates almost all the salt-affected area was situated in relatively lower slope areas exhibiting the flat to the almost flat slope (0–2%) (Fig. 5). Salt-affected areas dominantly cover the flat terrain of the studied area around Abaya and Chamo Lakes South Ethiopia Rift Valley [72,82]. During the high rainy season, the runoff collected from the surrounding elevated and steep topography landform of Gamo highlands area and flooded the flat terrains of around the Abaya and Chamo Lakes [129,130]. These areas developed on almost flat to flat landforms (0–2%) and sometimes Sile, Elgo, Hare, Baso, and Kulfo Rivers overflowed and flooded the area during the high rainy season. It is prone to flooding during the rainy season. The result suggested that landform in the study area may influence the pattern and magnitude of spatial variability in salinity and sodicity of the study area. The lower elevation areas were very susceptible to soil salinization, whereas the higher had the least influence on the process [131,132]. Excessive evaporation and low-lying topography could be some of the factors responsible for the rising of soil salinity and sodicity at the lower elevations [133]. This is probably because if the land had high fine particles with poor drainage it allows soluble salts within the irrigation waters to accumulate in soil profiles and increase the salt concentration on the soil surface and then, evaporation selectively removes the waters and leaves soluble salts on the soil [134,135]. The result is supported by the findings of [19] that their study area with low laying land form and area with shallow water table are greatly affected by salinity. Similarly low-lying topography and poor vegetation cover greatly enhanced the salinization [136,137]. [19] also confirmed that salt accumulation is more prevalent in low-lying landforms with relatively low elevations than in relatively steep landform areas.

3.6. Recommended reclamation strategies of the studied agricultural salt-affected soils

It is important to note that the recommendations for soil remediation vary depending on the site's specific conditions, including the

Table 4
Salt-affected soils type of salt class and areas concerning sampling sites.

Sampling Sites	Salt-affected soils type of salt class and area					
Omo Lante	Type of salt class	SSO	S	NSNSO	–	Total area
	Area(ha)	0.62	1.02	558.01	–	559.65
	Area (%)	0.11	0.18	99.71	–	100
Lante	Type of salt class	NSNSO	SO	S	SSO	Total area
	Area (ha)	0.02	0.01	0.01	228.77	228.81
	Area (%)	0.01	0	0	99.98	100
Abulo	Type of salt class	SO	S	NSNSO	SSO	Total area
	Area (ha)	0.2	10.78	419.41	6.5	436.9
	Area (%)	0.05	2.47	96	1.49	100
G/Kanchama	Type of salt class	S	SSO	SO	NSNSO	Total area
	Area (ha)	0.76	352.69	249.51	19.32	622.28
	Area (%)	0.12	56.68	40.1	3.11	100
Z/Elgo	Type of salt class	S	SSO	NSNSO	SO	Total area
	Area(ha)	1.59	4.99	420	0.43	427.01
	Area (%)	0.37	1.17	98.36	0.1	100

Where: S= Saline, SO = Sodic, SSO= Saline Sodic, NSNSO = Non-saline non-sodic.

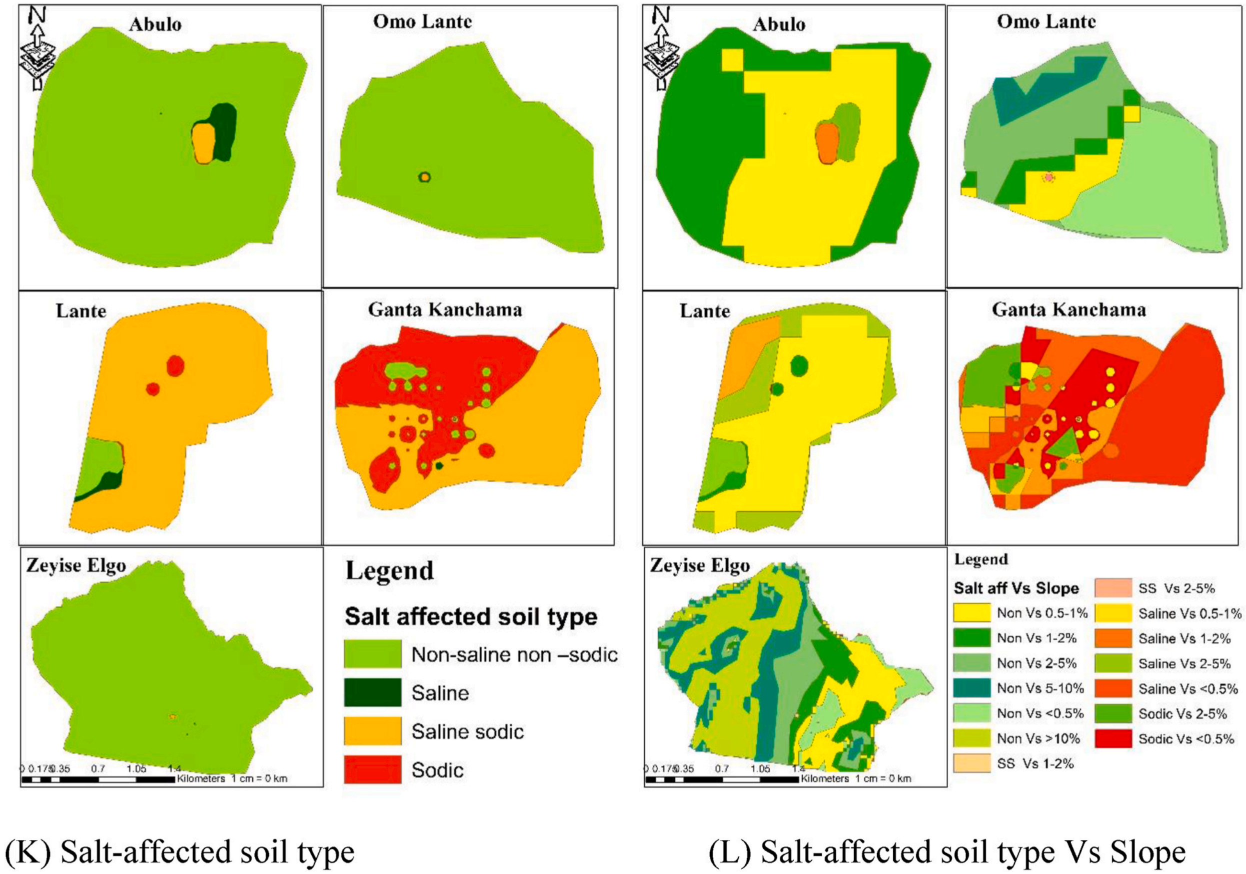

Fig. 5. This figure displays the salt-affected soil type and spatial distribution and salt-affected soil versus landform (slope) concerning all sampling sites of the study area, respectively. Where (K) Salt-affected soil type represented each sampling site's salt-affected soil type, (L) Salt-affected soil type vs. slope represented the salt-affected soil type and distribution concerning landform.

type and severity of salt-affectedness, the availability of water resources, and the cost of different remediation options [138–140]. In general, leaching with irrigation water of high quality removes salts from the soil effectively. However, this can be expensive and time-consuming, especially in areas with limited water resources [141–143]. Amendments with organic matter, such as compost or manure, chemical amendments (gypsum), and phytoremediation can also help improve soil structure and drainage, reducing salt accumulation. The Omo Lante, Abulo, and Zyise Elgo sites recommend leaching with good-quality irrigation water. In contrast, the Lante and Ganta Kanchama sites suggest amendment with organic matter and chemicals (gypsum) and recommend leaching with good-quality irrigation water (Fig. 6). Farmers should consult with soil science experts for a specific remediation plan. Additional tips include drip irrigation, planting salt-tolerant crops, avoiding over-fertilization, and monitoring soil salinity levels.

4. Conclusion

The major land degradation mechanisms and agricultural productivity reduction have been recognized as soil sodication and salinization. Alkaline soil reactions dominated the study area. Soils were generally categorized as free of excess salt, having no adverse effect on the growth and productivity of most crops. The spatial interpolation result in exchangeable sodium percentage (ESP) suggested that the area is dominated by low to high-risk soil sodicity and a noticeable variation in the exchangeable sodium value distribution within the research area and overwhelmed with high rates. The current study reveals a wide range of spatial heterogeneity in terms of types and severity among different salt-affected soil classes, implying that site-specific reclamation measures are required to address the studied area's current salinity and sodicity problems. The study area should be prevented, monitored, and implemented by using appropriate salt-affected soil reclamation measures to sustain soil productivity in the studied area. Generally, amendments with organic matter, such as compost or manure, chemical amendments (gypsum), and phytoremediation can also help improve soil structure and drainage, reducing salt accumulation. It is advised that soluble salts be leached using high-quality irrigation water on the Omo Lante, Abulo, and Zyise Elgo sites. Meanwhile, the Lante and Ganta Kanchama sites advocate amending salinity and sodicity with organic matter and chemicals (gypsum) and leaching high-quality irrigation water. Farmers must consult a soil science expert to develop an appropriate reclamation strategy.

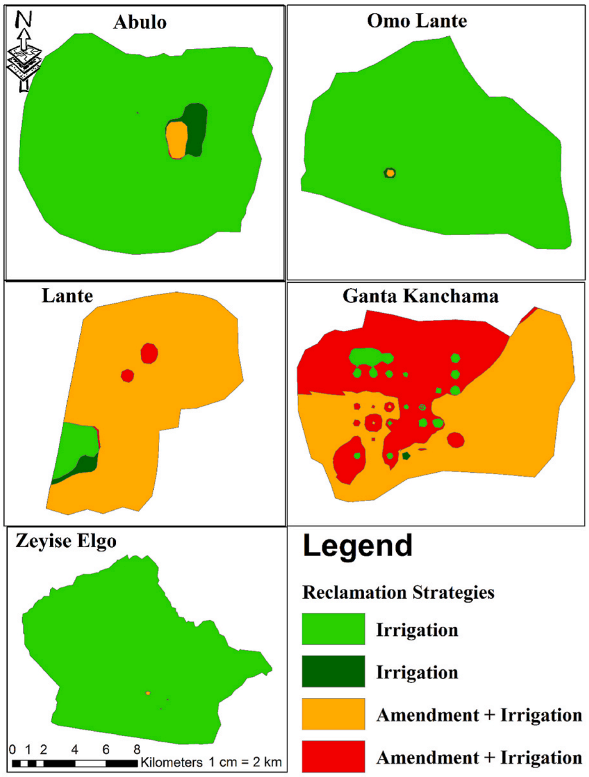

(M) Reclamation strategies

Fig. 6. This figure illustrates the map of recommended reclamation strategies of the studied agricultural salt-affected soils concerning all sampling sites in the area around Abaya and Chamo Lakes South Ethiopia Rift Valley (where amendment represented organic matter (compost or manure), chemical amendments (gypsum), and phytoremediation to reclaim salt-affected soils, irrigation represented good quality irrigation water for leaching soluble salts).

Funding

Under the Interuniversity Cooperation (IUC) program with the Arba Minch University (AMU) of Ethiopia, VLIR-UOS Belgium funded the study under the "Reducing land degradation through and for sustainable rural land use research" project (AMUE-T2017IUC035A101). The study work was financially supported by the Arba Minch University Research Directorate and the Ethiopian Ministry of Education under the Ph.D. subsidiary grants

Data availability statement

No data has been deposited into a publicly available repository; hence, it will be available upon request.

CRediT authorship contribution statement

Azmera Walche: Writing – original draft, Visualization, Validation, Software, Methodology, Investigation, Formal analysis, Data curation, Conceptualization. **Wassie Haile:** Writing – review & editing, Visualization, Supervision, Methodology, Data curation. **Alemayehu Kiflu:** Writing – original draft, Visualization, Validation, Supervision, Data curation. **Dereje Tsegaye:** Writing – review & editing, Visualization, Validation, Supervision, Data curation.

Declaration of competing interest

The authors declare the following financial interests/personal relationships which may be considered as potential competing interests:Azmra Walche reports VLIR-UOS Belgium provided financial support to fund the study under the "Reducing land degradation through and for sustainable rural land use research project in South Ethiopia Rift Valley" (AMUET2017IUC 035A101), by the Arba Minch University Research Directorate and the Ethiopian Ministry of Education under the Ph.D. subsidiary grants. If there are other authors, they declare that any known competing financial interests or personal relationships could have influenced none of the works reported in this study.

Acknowledgments

The authors thank the individuals and organizations that helped and supported them throughout their study. The authors thank Biruk Zewudie and Biruk Alemneh for supporting QGIS works and Samson Tsegaye's assistance in the field and the lab. The authors express their gratitude to Arba Minch University's Water Supply and Environmental Engineering, Civil Engineering Laboratory, and lab personnel for all the resources and assistance they offered. They also thank the Ethiopia Design and Water Works soil laboratory, the Engineering Corporation of Oromia in Addis Ababa, and the lab staff for their efforts. Lastly, the authors thank Arba Minch University for logistical support for the study.

Appendix A. Supplementary data

Supplementary data to this article can be found online at https://doi.org/10.1016/j.heliyon.2024.e33410.

References

[1] J.C. Dagar, R.K. Yadav, A. Singh, N.T. Singh, Historical perspectives and dynamics of nature, extent, classification and management of salt-affected soils and waters, Res. Dev. Saline Agric. (2019) 3–52.
[2] K. Negacz, Ž. Malek, A. de Vos, P. Vellinga, Saline soils worldwide: identifying the most promising areas for saline agriculture, J. Arid Environ. 203 (2022) 104775.
[3] FAO, Mapping of Salt-Affected Soils: Technical Manual, 2020, https://doi.org/10.4060/ca9215en. Rome: Rome, FAO.
[4] R. Chhabra, R. Chhabra, Nutrient management in salt-affected soils, Salt-affected Soils Marg. Waters Glob. Perspect. Sustain. Manag. (2021) 349–429.
[5] A. Adane, H. Gebrekidan, K. Kibret, Effects of treatment application rates (fym and gypsum) on selected chemical properties of saline sodic soils under water limited condition in eastern lowlands Ethiopia, For. Res. Eng. Int. J. e 3 (3) (2019) 106–113, https://doi.org/10.15406/freij.2019.03.00086.
[6] A.W. Daba, A.S. Qureshi, Review of Soil Salinity and Sodicity Challenges to Crop Production in the Lowland Irrigated Areas of Ethiopia and its, 2021.
[7] K. Ivushkin, H. Bartholomeus, A.K. Bregt, A. Pulatov, B. Kempen, L. De Sousa, Global mapping of soil salinity change, Remote Sens. Environ. 231 (2019) 111260.
[8] B. Okur, N. Örçen, Soil salinization and climate change, in: Climate Change and Soil Interactions, Elsevier, 2020, pp. 331–350.
[9] R. Prăvălie, Drylands extent and environmental issues. A global approach, Earth-Science Rev. 161 (2016) 259–278.
[10] K. Alemayehu, B. Sheleme, J. Schoenau, Characterization of problem soils in and around the south central Ethiopian Rift Valley, J. Soil Sci. Environ. Manag. 7 (11) (2016) 191–203.
[11] M. Asmamaw, A. Haile, G. Abera, Characterization and classification of salt affected soils and irrigation water in Tendaho sugarcane production farm, North-Eastern Rift Valley of Ethiopia, African J. Agric. Res. 13 (9) (2018) 403–411.
[12] A. Habtamu, H. Wassie, Review on causes and management strategies of salt affected soils in lowlands of Ethiopia, Arch. Crop Sci. 5 (2) (2022) 1–7, https://doi.org/10.36959/718/615.
[13] A. Walche, W. Haile, A. Kiflu, D. Tsegaye, Assessment and characterization of agricultural salt-affected soils around Abaya and Chamo lakes, south Ethiopia Rift Valley, Appl. Environ. Soil Sci. 2023 (2023) 1–18, https://doi.org/10.1155/2023/3946508.
[14] G. Ondrasek, Z. Rengel, Environmental salinization processes: detection, implications & solutions, Sci. Total Environ. 754 (2021) 142432.
[15] A. Parvaiz, J.A. Khattak, I. Hussain, N. Masood, T. Javed, A. Farooqi, Salinity enrichment, sources and its contribution to elevated groundwater arsenic and fluoride levels in Rachna Doab, Punjab Pakistan: Stable isotope (δ2H and δ18O) approach as an evidence, Environ. Pollut. 268 (2021) 115710.
[16] N. Tessema, D. Yadeta, A. Kebede, G.T. Ayele, Soil and irrigation water salinity, and its consequences for agriculture in Ethiopia: a systematic review, Agric. For. 13 (1) (2023), https://doi.org/10.3390/agriculture13010109.
[17] X. Yin, et al., An interplay of soil salinization and groundwater degradation threatening coexistence of oasis-desert ecosystems, Sci. Total Environ. 806 (2022) 150599.
[18] S.M.S. Shokri-Kuehni, B. Raaijmakers, T. Kurz, D. Or, R. Helmig, N. Shokri, Water table depth and soil salinization: from pore-scale processes to field-scale responses, Water Resour. Res. 56 (2) (2020) e2019WR026707.
[19] S. Zewdu, K. V Suryabhagavan, M. Balakrishnan, Geo-spatial approach for soil salinity mapping in sego irrigation farm, south Ethiopia, J. Saudi Soc. Agric. Sci. 16 (1) (2017) 16–24.
[20] X. Yin, et al., Assessment and mechanism analysis of plant salt tolerance regulates soil moisture dynamics and controls root zone salinity and sodicity in seasonally irrigated agroecosystems, J. Hydrol. 617 (2023) 129138.
[21] A. Singh, Poor-drainage-induced salinization of agricultural lands: management through structural measures, Land Use Pol. 82 (2019) 457–463.
[22] H. Daneshmand, S. Alaghmand, M. Camporese, A. Talei, P.J.-F. Yeh, E. Daly, Long-term impacts of partial afforestation on water and salt dynamics of an intermittent catchment under climate change, Water 12 (4) (2020) 1067.
[23] J.W. Hopmans, et al., Critical knowledge gaps and research priorities in global soil salinity, Adv. Agron. 169 (2021) 1–191.
[24] C.S.S. Ferreira, S. Seifollahi-Aghmiuni, G. Destouni, N. Ghajarnia, Z. Kalantari, Soil degradation in the European Mediterranean region: processes, status and consequences, Sci. Total Environ. 805 (2022) 150106.
[25] A. Nyéki, et al., Application of spatio-temporal data in site-specific maize yield prediction with machine learning methods, Precis. Agric. 22 (2021) 1397–1415.
[26] C.T. Omuto, et al., Digital soil assessment in support of a soil information system for monitoring salinization and sodification in agricultural areas, L. Degrad. Dev. 33 (8) (2022) 1204–1218.
[27] E. Günal, Delineating reclamation zones for site-specific reclamation of saline-sodic soils in Dushak, Turkmenistan, PLoS One 16 (8) (2021) e0256355.
[28] A. Singh, Soil salinity: a global threat to sustainable development, Soil Use Manag. 38 (1) (2022) 39–67.
[29] S. Laiskhanov, Z. Smanov, K. Kaimuldinova, D. Aliaskarov, N. Myrzaly, Study of the ecological and reclamation condition of abandoned saline lands and their development for sustainable development goals, Sustainability 15 (19) (2023) 14181.
[30] G. Aredehey, H. Libsekal, M. Brhane, K. Welde, A. Giday, Top-soil salinity mapping using geostatistical approach in the agricultural landscape of Timuga irrigation scheme, South Tigray, Ethiopia, Cogent Food Agric. 4 (1) (2018) 1514959.
[31] M.A. Oliver, R. Webster, Basic Steps in Geostatistics: the Variogram and Kriging, Springer, 2015.
[32] T. Tiruneh, Water Quality Monitoring in Lake Abaya and Lake Chamo Region, vol. 8, 2005, p. 362.
[33] D. Abdi, S. Gebrekristos, Regionalization of low flow analysis in data scarce region: the case of the lake abaya-chamo sub-basin, Rift Valley Lakes basin, Ethiopia, J. Water Manag. Model. (2022).
[34] H.A. Mengistu, M.B. Demlie, T.A. Abiye, Groundwater Resource Potential and Status of Groundwater Resource Development in Ethiopia, 2019.
[35] M. Delbari, P. Afrasiab, B. Gharabaghi, M. Amiri, A. Salehian, Spatial variability analysis and mapping of soil physical and chemical attributes in a salt-affected soil, Arab. J. Geosci. 12 (2019) 1–18.

[36] R. Srinivasan, M. Lalitha, M. Chandrakala, S. Dharumarajan, R. Hegde, Application of remote sensing and GIS techniques in assessment of salt affected soils for management in large scale soil survey, in: Soil Health and Environmental Sustainability: Application of Geospatial Technology, Springer, 2022, pp. 131–161.
[37] M.K. Abdel-Fattah, A GIS-based approach to identify the spatial variability of salt affected soil properties and delineation of site-specific management zones: a case study from Egypt, Soil Sci. Annu. 71 (1) (2020) 76–85.
[38] M.E. Guntiñas, M.C. Leirós, C. Trasar-Cepeda, F. Gil-Sotres, Effects of moisture and temperature on net soil nitrogen mineralization: a laboratory study, Eur. J. Soil Biol. 48 (2012) 73–80.
[39] G.E. Rayment, D.J. Lyons, Soil Chemical Methods: Australasia, vol. 3, CSIRO publishing, 2011.
[40] J.J. Miller, D. Curtin, Electrical conductivity and soluble ions, Soil Sampl. methods Anal. 2 (2006).
[41] S. Dasgupta, S. Sengupta, S. Saha, A. Sarkar, K.C. Anantha, Approaches in advanced soil elemental extractability: catapulting future soil–plant nutrition research, Soil Sci. Fundam. to Recent Adv. (2021) 191–236.
[42] D.J. Walker, M.P. Bernal, The effects of olive mill waste compost and poultry manure on the availability and plant uptake of nutrients in a highly saline soil, Bioresour. Technol. 99 (2) (2008) 396–403.
[43] L.A. Richards, et al., Diagnosis and improvement of saline and alkali soils, Soil Sci. Soc. Am. J. 18 (February 1954) 348, 1954.
[44] R. Burt, Soil Survey Laboratory Information Manual, United States Department of Agriculture, Natural Resources Conservation …, 2011.
[45] X. Li, S.X. Chang, K.F. Salifu, Soil texture and layering effects on water and salt dynamics in the presence of a water table: a review, Environ. Rev. 22 (1) (2014) 41–50.
[46] N. Wang, J. Xue, J. Peng, A. Biswas, Y. He, Z. Shi, Integrating remote sensing and landscape characteristics to estimate soil salinity using machine learning methods: a case study from Southern Xinjiang, China, Remote Sens 12 (24) (2020) 4118.
[47] I. Stavi, N. Thevs, S. Priori, Soil salinity and sodicity in drylands: a review of causes, effects, monitoring, and restoration measures, Front. Environ. Sci. (2021) 330.
[48] B.L. Yusuf, A. Mustapha, M.A. Yusuf, M. Ahmed, Soil salinity assessment using geostatistical models in some parts of Kano River Irrigation Project Phase I (KRPI), Model. Earth Syst. Environ. 6 (2020) 2225–2234.
[49] J. Nyengere, Y. Okamoto, S. Funakawa, H. Shinjo, Analysis of Spatial Heterogeneity of Soil Physicochemical Properties in Northern Malawi, Geoderma Reg., 2023 e00733.
[50] M.J. Blanca Mena, R. Alarcón Postigo, J. Arnau Gras, R. Bono Cabré, R. Bendayan, Non-normal data: is ANOVA still a valid option? Psicothema 29 (4) (2017) 552–557, 2017.
[51] R. Terefe, K. yong Yu, Y. Deng, X. Yao, F. Wang, J. Liu, Spatial variability of soil chemical properties of Moso bamboo forests of China, J. For. Res. 32 (6) (2021) 2599–2608, https://doi.org/10.1007/s11676-020-01251-2.
[52] C. Takele, B. Iticha, Use of infrared spectroscopy and geospatial techniques for measurement and spatial prediction of soil properties, Heliyon 6 (10) (2020) e05269.
[53] H.N. Pahalvi, L. Rafiya, S. Rashid, B. Nisar, A.N. Kamili, Chemical fertilizers and their impact on soil health, Microbiota Biofertilizers, Vol 2 Ecofriendly Tools Reclam. Degrad. Soil Environs (2021) 1–20.
[54] L. Wogi, N. Dechassa, B. Haileselassie, F. Mekuria, A. Abebe, L. Tamene, A guide to standardized methods of analysis for soil , water , plant , and fertilizer resources for data documentation and knowledge sharing in Ethiopia, Int. Cent. Trop. Agric. (519) (2021) 41.
[55] J.R. Landon, Booker Tropical Soil Manual: a Handbook for Soil Survey and Agricultural Land Evaluation in the Tropics and Subtropics, Routledge, 2014.
[56] N. Marcar, Prospects for managing salinity in Southern Australia using trees on farmland, Agrofor. Manag. waterlogged saline soils poor-quality waters (2016) 49–71.
[57] Y. Fei, D. She, K. Fang, Identifying the main factors contributing to the spatial variability of soil saline–sodic properties in a reclaimed coastal area, Vadose Zo. J. 17 (1) (2018) 1–11.
[58] S. Sani, A. Abdulkadir, S.A. hmad Pantami, M. Sani, A.M. Amin, M.Y. Abdullahi, Spatial variability and mapping of selected soil physical properties under continuous cultivation, Turkish J. Agric. Sci. Technol. 11 (4) (2023) 719–729.
[59] H.K. Addis, A. Klik, S. Strohmeier, Spatial variability of selected soil attributes under agricultural land use system in a mountainous watershed, Ethiopia, Int. J. Geosci. 6 (6) (2015) 605.
[60] S. Lin, et al., Spatiotemporal variability of soil physical properties and water, salt, nitrogen, and phosphorus contents for farm level, Can. J. Soil Sci. (2023).
[61] X. Shi, et al., Impact of saline soil improvement measures on salt content in the abandonment-reclamation process, Soil Tillage Res. 208 (2021) 104867.
[62] N. Shahinzadeh, T. Babaeinejad, K. Mohsenifar, N. Ghanavati, Spatial variability of soil properties determined by the interpolation methods in the agricultural lands, Model. Earth Syst. Environ. 8 (4) (2022) 4897–4907.
[63] Y. Jing, H. Zhu, H. Ding, R. Bi, Spatial variation in soil available potassium and temporal changes due to intrinsic and extrinsic factors: a 10-year study, J. Soil Sci. Plant Nutr. (2022) 1–10.
[64] X. Yao, K. Yu, Y. Deng, J. Liu, Z. Lai, Spatial variability of soil organic carbon and total nitrogen in the hilly red soil region of Southern China, J. For. Res. 31 (6) (2020) 2385–2394.
[65] L. Ye, W. Tan, L. Fang, L. Ji, H. Deng, Spatial Analysis of Soil Aggregate Stability in a Small Catchment of the Loess Plateau, China: I. Spatial Variability, vol 179, Soil Tillage Res., 2018, pp. 71–81.
[66] A. Abdu, F. Laekemariam, G. Gidago, A. Kebede, L. Getaneh, Variability analysis of soil properties, mapping, and crop test responses in Southern Ethiopia, Heliyon 9 (3) (2023) e05269.
[67] A.M. Saleh, Spatial variability mapping of some soil properties in Jadwal Al_Amir Project/Babylon/Iraq, J. Indian Soc. Remote Sens. 46 (9) (2018) 1481–1495.
[68] B.S. Some'e, F. Hassanpour, A. Ezani, S.R. Miremadi, H. Tabari, Investigation of spatial variability and pattern analysis of soil properties in the northwest of Iran, Environ. Earth Sci. 64 (2011) 1849–1864.
[69] B. Takoutsing, G.B.M. Heuvelink, Comparing the prediction performance, uncertainty quantification and extrapolation potential of regression kriging and random forest while accounting for soil measurement errors, Geoderma 428 (2022) 116192.
[70] R. Nogueira Martins, F. Ferreira Lima Dos Santos, G. De Moura Araújo, L. De Arruda Viana, J.T. Fim Rosas, Accuracy assessments of stochastic and deterministic interpolation methods in estimating soil attributes spatial variability, Commun. Soil Sci. Plant Anal. 50 (20) (2019) 2570–2578.
[71] L.A. Richards, Diagnosis and improvement of saline and alkali soils, LWW 78 (2) (1954).
[72] A.L. Bassa, T. Kasa, D. Reddythota, G.T. Negatu, Investigation on the source of soil salinity in agricultural land adjacent to Chamo Lake, Ethiopia, Water, Air, Soil Pollut. 234 (9) (2023) 576.
[73] C. Mukungurutse, N. Nyapwere, A. Manyanga, L. Mhaka, Pedological characterization and classification of typical soils of Lupane District, Zimbabwe, Int J Plant Soil Sci. (2018), https://doi.org/10.9734/ijpss/2018/39609.
[74] P.D. Sreedevi, P.D. Sreekanth, S. Ahmed, D. V Reddy, Evaluation of groundwater quality for irrigation in a semi-arid region of South India, Sustain. Water Resour. Manag. 5 (2019) 1043–1056.
[75] L. Bortolini, C. Maucieri, M. Borin, A tool for the evaluation of irrigation water quality in the arid and semi-arid regions, Agronomy 8 (2) (2018) 23.
[76] M.A. Abdennour, et al., Geochemical characterization of the salinity of irrigated soils in arid regions (Biskra, SE Algeria), Acta Geochim 40 (2021) 234–250.
[77] L.N. Allen, J.W. MacAdam, Irrigation and water management, Forages Sci. Grassl. Agric. 2 (2020) 497–513.
[78] P.S. Minhas, T.B. Ramos, A. Ben-Gal, L.S. Pereira, Coping with salinity in irrigated agriculture: crop evapotranspiration and water management issues, Agric. Water Manag. 227 (2020) 105832.
[79] A. Regassa, K. Kibret, Y.G. Selassie, A. Kiflu, W. Tena, Soil properties, in: The Soils of Ethiopia, Springer, 2023, pp. 111–156.
[80] R. Moirana, Remediation of Soils Contaminated with Fluoride Using Seaweed-Derived Materials: Case of Slopes of Mount Meru, NM-AIST, 2023.
[81] P. Van Straaten, Rocks for Crops: Agrominerals of Sub-saharan Africa, 2002.
[82] D.A. Zebire, T. Ayele, M. Ayana, Characterizing soils and the enduring nature of land uses around the Lake Chamo Basin in South-West Ethiopia, J. Ecol. Environ. 43 (1) (2019) 1–32.

[83] B. Bedadi, S. Beyene, T. Erkossa, E. Fekadu, Soil management, in: The Soils of Ethiopia, Springer, 2023, pp. 193–234.
[84] R.M.A. Machado, R.P. Serralheiro, Soil salinity: effect on vegetable crop growth. Management practices to prevent and mitigate soil salinization, Horticulturae 3 (2) (2017) 30.
[85] T. Tugwell-Wootton, G. Skrzypek, S. Dogramaci, J. McCallum, P.F. Grierson, Soil moisture evaporative losses in response to wet-dry cycles in a semiarid climate, J. Hydrol. 590 (2020) 125533.
[86] N.N. Mohamed, Management of Salt-Affected Soils in the Nile Delta, Nile Delta, 2017, pp. 265–295.
[87] R. Chhabra, Salt-affected Soils and Marginal Waters: Global Perspectives and Sustainable Management, Springer Nature, 2022.
[88] Z.M. Al-Ali, A. Bannari, H. Rhinane, A. El-Battay, S.A. Shahid, N. Hameid, Validation and comparison of physical models for soil salinity mapping over an arid landscape using spectral reflectance measurements and Landsat-OLI data, Remote Sens 13 (3) (2021) 494.
[89] B. Hailu, H. Mehari, Impacts of soil salinity/sodicity on soil-water relations and plant growth in dry land areas: a review, J. Nat. Sci. Res. 12 (3) (2021) 1–10.
[90] Kumar, P.K. Sharma, Soil salinity and food security in India, Front. Sustain. Food Syst. 4 (2020) 533781.
[91] R. Tirado-Corbalá, B.K. Slater, W.A. Dick, J. Bigham, M. Muñoz-Muñoz, Gypsum amendment effects on micromorphology and aggregation in no-till Mollisols and Alfisols from western Ohio, USA, Geoderma Reg. 16 (2019) e00217.
[92] F. Javaheri, I. Esfandiarpour-Boroujeni, M.H. Farpoor, D. Holthusen, R.D. Stewart, Counterions, smectite, and palygorskite increase microstructural stability of saline-sodic soils, Soil Tillage Res. 216 (2022) 105258.
[93] F. Bergaya, M. Jaber, J. Lambert, Clays and clay minerals, Rubber-Clay Nanocomposites Sci. Technol. Appl. (2011) 1–44.
[94] P. Gangwar, R. Singh, M. Trivedi, R.K. Tiwari, Sodic soil: management and reclamation strategies, Environ. Concerns Sustain. Dev. 2 (2020) 175–190. Biodiversity, Soil Waste Manag.
[95] A. Tomaz, et al., Risk assessment of irrigation-related soil salinization and sodification in Mediterranean areas, Water 12 (12) (2020) 3569.
[96] Z. Mohammad, S.A. Shahid, L. Heng, S.A. Shahid, M. Zaman, L. Heng, Salinity and sodicity adaptation and mitigation options, Guidel. Salin. assessment, Mitig. Adapt. using Nucl. Relat. Tech (2018) 55–89.
[97] M. Zaman, S.A. Shahid, L. Heng, S.A. Shahid, M. Zaman, L. Heng, Introduction to soil salinity, sodicity and diagnostics techniques, Guidel. Salin. assessment, Mitig. Adapt. using Nucl. Relat. Tech (2018) 1–42.
[98] A. Mohanavelu, S.R. Naganna, N. Al-Ansari, Irrigation induced salinity and sodicity hazards on soil and groundwater: an overview of its causes, impacts and mitigation strategies, Agriculture 11 (10) (2021) 983.
[99] I.E. Olorunfemi, J.T. Fasinmirin, F.F. Akinola, Soil physico-chemical properties and fertility status of long-term land use and cover changes: a case study in Forest vegetative zone of Nigeria, Eurasian J. Soil Sci. 7 (2) (2018) 133–150.
[100] M. Qadir, S. Schubert, Degradation processes and nutrient constraints in sodic soils, L. Degrad. Dev. 13 (4) (2002) 275–294.
[101] B. Huang, Waterlogging responses and interaction with temperature, salinity, and nutrients, Plant-environment Interact 77 (2000) 263.
[102] A. Syed, G. Sarwar, S.H. Shah, S. Muhammad, Soil salinity research in 21st century in Pakistan: its impact on availability of plant nutrients, growth and yield of crops, Commun. Soil Sci. Plant Anal. 52 (3) (2021) 183–200.
[103] S. Rajendiran, M.L. Dotaniya, M.V. Coumar, N.R. Panwar, J.K. Saha, Heavy metal polluted soils in India: status and countermeasures, JNKVV Res. J. 49 (3) (2015) 320–337.
[104] M.A.E. AbdelRahman, An overview of land degradation, desertification and sustainable land management using GIS and remote sensing applications, Rend. Lincei. Sci. Fis. e Nat. (2023) 1–42.
[105] M.V.K. Sivakumar, Interactions between climate and desertification, Agric. For. Meteorol. 142 (2–4) (2007) 143–155.
[106] Z. Noori, M.A. Delavar, Y. Safari, S.M. Alavi-Siney, Reclamation of a calcareous sodic soil with combined amendments: interactive effects of chemical and organic materials on soil chemical properties, Arab. J. Geosci. 14 (2021) 1–11.
[107] V.K. Yadav, et al., The processing of calcium rich agricultural and industrial waste for recovery of calcium carbonate and calcium oxide and their application for environmental cleanup: a review, Appl. Sci. 11 (9) (2021) 4212.
[108] D.A. Horneck, J.W. Ellsworth, B.G. Hopkins, D.M. Sullivan, R.G. Stevens, Managing Salt-Affected Soils for Crop Production, 2007.
[109] M.D. Meena, et al., Municipal solid waste (MSW): strategies to improve salt affected soil sustainability: a review, Waste Manag. 84 (2019) 38–53.
[110] F. Ranjbar, M. Jalali, The effect of chemical and organic amendments on sodium exchange equilibria in a calcareous sodic soil, Environ. Monit. Assess. 187 (2015) 1–21.
[111] H.S. Kim, K.-R. Kim, S.-H. Lee, A. Kunhikrishnan, W.-I. Kim, K.-H. Kim, Effect of gypsum on exchangeable sodium percentage and electrical conductivity in the Daeho reclaimed tidal land soil in Korea—a field scale study, J. Soils Sediments 18 (2018) 336–341.
[112] D.B. Watts, W.A. Dick, Sustainable uses of FGD gypsum in agricultural systems: introduction, J. Environ. Qual. 43 (1) (2014) 246–252.
[113] S.M. Zoca, C. Penn, An important tool with no instruction manual: a review of gypsum use in agriculture, Adv. Agron. 144 (2017) 1–44.
[114] A.K. Rai, N. Basak, P. Sundha, Chemistry of salt-affected soils, Salin. Manag. India. Cent. Soil Salin. Res. Institute, Karnal, Haryana (2020) *(Submitted to ICAR, New Delhi)*.
[115] S.C. Bhatla, M.A. Lal, R. Kathpalia, S.C. Bhatla, Plant mineral nutrition, Plant Physiol. Dev. Metab. (2018) 37–81.
[116] D. Kumaragamage, J. Warren, G. Spiers, Soil chemistry, Digging into Can. Soils (2021).
[117] N. Kumari, C. Mohan, Basics of clay minerals and their characteristic properties, Clay Clay Min. 24 (2021) 1–29.
[118] H. Abbaslou, A. Abtahi, F.J.M. Peinado, H. Owliaie, F. Khormali, Mineralogy and characteristics of soils developed on Persian Gulf and Oman sea basin, southern Iran: implications for soil evolution in relation to sedimentary parent material, Soil Sci. 178 (10) (2013) 568–584.
[119] G.B. Tesfahunegn, L. Tamene, P.L.G. Vlek, Catchment-scale spatial variability of soil properties and implications on site-specific soil management in northern Ethiopia, Soil Tillage Res. 117 (2011) 124–139.
[120] D. Panday, R.B. Ojha, D. Chalise, S. Das, B. Twanabasu, Spatial variability of soil properties under different land use in the Dang district of Nepal, Cogent Food Agric. 5 (1) (2019) 1600460.
[121] V.C. Smith, P.G. Albert, An introduction to tephrochronology and the correlation of sedimentary sequences using volcanic ash layers, Handb. Archaeol. Sci. 1 (2023) 133–149.
[122] S.F. EL-Gioushy, A.S.A. Abd-El-Rahman, K.R. Islam, R.M.Y. Zewail, Growth, yield and fruit quality of specialty banana in response to yeast extract and potassium amendments, J. Plant Nutr. 45 (7) (2022) 1017–1029.
[123] M.L. Dotaniya, V.D. Meena, B.B. Basak, R.S. Meena, Potassium uptake by crops as well as microorganisms, Potassium solubilizing Microorg. Sustain. Agric. (2016) 267–280.
[124] S. Fischer, et al., Soil and farm management effects on yield and nutrient concentrations of food crops in East Africa, Sci. Total Environ. 716 (2020) 137078.
[125] A.M. Stefanowicz, P. Kapusta, S. Zubek, M. Stanek, M.W. Woch, Soil organic matter prevails over heavy metal pollution and vegetation as a factor shaping soil microbial communities at historical Zn–Pb mining sites, Chemosphere 240 (2020) 124922.
[126] Z. Haj-Amor, S. Bouri, Subsurface drainage system performance, soil salinization risk, and shallow groundwater dynamic under irrigation practice in an arid land, Arab. J. Sci. Eng. 44 (2019) 467–477.
[127] J. Kakeh, M. Gorji, M.H. Mohammadi, H. Asadi, F. Khormali, M. Sohrabi, Effect of biocrusts on profile distribution of soil water content and salinity at different stages of evaporation, J. Arid Environ. 191 (2021) 104514.
[128] G. Gebremeskel, T.G. Gebremicael, M. Kifle, E. Meresa, T. Gebremedhin, A. Girmay, Salinization pattern and its spatial distribution in the irrigated agriculture of Northern Ethiopia: an integrated approach of quantitative and spatial analysis, Agric. Water Manag. 206 (2018) 147–157.
[129] T.C. Digga, River Channel Stability Analysis and Mitigation Measures (Case of Kulfo River, Gamo Zone, Southern, Ethiopia), 2023.
[130] B.W. Gindi, Impact of land use/land cover and climate change on soil erosion, in: Sile Watershed, Lake Abaya-Chamo Sub-Basin, Southern Ethiopia, 2022.
[131] J. Peng, et al., Estimating soil salinity from remote sensing and terrain data in southern Xinjiang Province, China, Geoderma 337 (2019) 1309–1319.
[132] D.L. Corwin, Climate change impacts on soil salinity in agricultural areas, Eur. J. Soil Sci. 72 (2) (2021) 842–862.
[133] D.L. Corwin, K. Yemoto, Salinity: electrical conductivity and total dissolved solids, Soil Sci. Soc. Am. J. 84 (5) (2020) 1442–1461.

[134] P.C. Moharana, R.S. Singh, S.K. Singh, B.L. Tailor, R.K. Jena, M.D. Meena, Development of secondary salinity and salt migration in the irrigated landscape of hot arid India, Environ. Earth Sci. 78 (2019) 1–11.
[135] A.C. Ortiz, L. Jin, Chemical and hydrological controls on salt accumulation in irrigated soils of southwestern US, Geoderma 391 (2021) 114976.
[136] Z.F. Hua, et al., Felsic volcanism as a factor driving the end-Permian mass extinction, Sci. Adv. 7 (47) (2021) eabh1390.
[137] Y. Zhang, et al., Characterization of soil salinization and its driving factors in a typical irrigation area of Northwest China, Sci. Total Environ. 837 (2022) 155808.
[138] B. Wicke, et al., Biomass production in agroforestry and forestry systems on salt-affected soils in South Asia: exploration of the GHG balance and economic performance of three case studies, J. Environ. Manage. 127 (2013) 324–334.
[139] B. Batidzirai, E.M.W. Smeets, A.P.C. Faaij, Harmonising bioenergy resource potentials—methodological lessons from review of state of the art bioenergy potential assessments, Renew. Sustain. Energy Rev. 16 (9) (2012) 6598–6630.
[140] L. Dhaouadi, et al., Agriculture sustainability in arid lands of southern Tunisia: ecological impacts of irrigation water quality and human practices, Irrig. Drain. 69 (5) (2020) 974–996.
[141] A. Javadi, B. Mostafazadeh-Fard, M. Shayannejad, M.R. Mosaddeghi, H. Ebrahimian, Soil physical and chemical properties and drain water quality as affected by irrigation and leaching managements, Soil Sci. Plant Nutr. 65 (4) (2019) 321–331.
[142] N.G. Mpela, Analysis of Antibiotics and PFAS as Potential Emerging Pollutants in the Water Bodies and Their Accumulation in Food Samples, 2021.
[143] M. Sultan, F. Ahmad, Irrigation and Drainage: Recent Advances, 2023.